Characterisation of cold-selective lamina I spinal projection neurons

Aimi N. Razlan[1,4], Wenhui Ma[1,4], Allen C. Dickie[1,4], Erika Polgár[1,4], Anna McFarlane[1], Mansi Yadav[1], Andrew H. Cooper[1], Douglas Strathdee[2], Masahiko Watanabe[3], Andrew M. Bell[1], Andrew J. Todd[1]*, Junichi Hachisuka[1]*

[1]School of Psychology and Neuroscience, College of Medical, Veterinary and Life Sciences, University of Glasgow, Glasgow G12 8QQ, UK

[2]School of Cancer Sciences, College of Medical, Veterinary and Life Sciences, University of Glasgow, Bearsden G61 1BD UK

[3]Department of Anatomy, Hokkaido University School of Medicine, Sapporo 060-8638, Japan

[4]Equal contribution

*Corresponding Authors: Andrew.Todd@glasgow.ac.uk and Junichi.Hachisuka@Glasgow.ac.uk

Click here to enter text.

ABSTRACT

Skin cooling is detected by primary afferents that express the Trpm8 channel, but how this information is conveyed to the brain remains poorly understood. We have previously identified a population of lamina I projection neurons belonging to the anterolateral system (ALS) that receive numerous contacts from Trpm8-expressing primary afferents. Here, using a semi-intact somatosensory preparation, we provide evidence that these cells correspond to the cold-selective ALS neurons identified in previous physiological studies. We also confirm the presence of synapses from Trpm8 afferents onto these cells at the ultrastructural level and with optogenetics. Based on our previous transcriptomic findings, we identify calbindin as a molecular marker, and show that this can be used to target the cold-selective ALS neurons for anterograde tracing studies. We provide evidence that they project to brain regions that have been implicated in thermosensation: the rostralmost part of the lateral parabrachial area, the caudal part of the periaqueductal grey matter, and the posterior triangular and ventral posterolateral nuclei of the thalamus. Our findings provide important insights into the organisation of neuronal circuits that underlie thermoregulation and the perception of cold stimuli applied to the skin.

Click here to enter text.

INTRODUCTION

The anterolateral system (ALS) consists of spinal cord neurons that project to various brain regions, including the caudal ventrolateral medulla (CVLM), the nucleus of the solitary tract (NTS), the lateral parabrachial area (LPB), the periaqueductal grey matter (PAG), the superior colliculus and the thalamus. ALS neurons are required for the perception of pain, itch and skin temperature, as shown by the loss of these sensations on the side contralateral to an anterolateral cordotomy[1,2]. Although axons belonging to this pathway ascend in the anterolateral quadrant in humans, they are located in the dorsolateral white matter in rodents[3-6]. ALS neurons account for only a small proportion (probably less than 1%) of spinal cord neurons[7,8] and are unevenly distributed, with a relatively high density in lamina I and the lateral spinal nucleus (LSN), and scattered cells in deeper laminae (III-VII) and around the central canal[9-12]. ALS neurons are functionally heterogeneous, and we recently identified 5 distinct transcriptomic populations, which we named ALS1-5[13]. This was based on single-nucleus RNA sequencing of a major subset of these cells, those that transiently express the transcription factor Phox2a during development[14].

Perception of skin cooling is dependent on primary afferent neurons that express the Trpm8 channel[15-19], and these terminate mainly in lamina I of the spinal cord[20-22]. Consistent with this, it has been shown that many lamina I projection neurons respond to cool or cold stimuli applied to the skin, with a distinctive subset of “cold-selective” neurons responding predominantly or exclusively to skin cooling[23-33].

How information is transmitted from Trpm8-expressing primary afferent neurons to these cold-selective lamina I ALS cells is currently not known, although a recent report has suggested that this occurs via a dedicated population of excitatory interneurons[34]. However, we had previously identified a population of lamina I ALS neurons that received dense synaptic input from Trpm8-expressing primary afferents[13]. These neurons had dendrites that were intimately associated with bundles of Trpm8-positive afferents, while their cell bodies generally also received numerous contacts, and were sometimes surrounded by these afferents. We therefore proposed that these cells correspond to the cold-selective neurons described above, and also provided evidence that they belonged to the ALS3 population[13].

The aims of this study were to characterise and validate the Trpm8^{Flp} mouse line that we had used to reveal this input, to confirm the presence of synaptic input, and to test the prediction that the lamina I projection neurons with dense synaptic input from Trpm8-

Click here to enter text.

expressing primary afferents do indeed correspond to the cold-selective population described in physiological studies[23-33]. In addition, since Calb1 (which encodes the calcium-binding protein calbindin) is one of the top differentially expressed genes in the ALS3 population, we used mice in which Cre recombinase is targeted to the Calb1 locus (Calb1^{Cre}) to investigate the projections of the ALS3 cells to the brain.

RESULTS

Validation of Trpm8^{Flp} mouse line and characterisation of Flp-expressing cells.

Trpm8^{Flp} mice were crossed with the Flp reporter line RCE:FRT to generate Trpm8^{Flp};RCE:FRT mice, in which cells that express Flp at any stage during development are labelled with GFP. Tissue was obtained from mice aged between 5-9 weeks for this part of the study. We used a stereological technique to quantify neurons in an L4 dorsal root ganglion (DRG) from 3 of these mice and found that 5.7% (range 5.4-6.7%) of all DRG neurons contained GFP (Figure 1A). We then performed fluorescence *in situ* hybridisation (FISH) to examine the extent of overlap between GFP and *Trpm8* mRNA (Figure 1B). In DRGs from 3 mice, we found that 92% (88%-98%) of GFP-containing cells had *Trpm8* message, while 83% (80%-86%) of cells with *Trpm8* were GFP-positive. These findings show a high degree of fidelity in the Trpm8^{Flp} line, and are consistent with the reported expression of *Trpm8* mRNA in 5-10% of mouse DRG cells[15]. We also used this tissue to determine the soma size of the GFP-positive cells (Figure 1C), and found that these were small, with a mean diameter of 14.6 µm (± 3.4 µm, SD), showing a very similar size range to that reported for cells captured with a different Trpm8^{Flp} mouse line[35]. Trpm8-positive cells that lacked GFP, as well as the few GFP-labelled cells that lacked *Trpm8* mRNA, showed a similar size distribution.

Transcriptomic studies have demonstrated that Trpm8-expressing primary afferents can co-express certain genes that serve as markers for primary afferent populations, such as Slc17a8 (which encodes Vglut3), Trpv1 and Tac1 (the gene coding for substance P), but lack other neuropeptides such as calcitonin gene-related peptide (CGRP) and somatostatin[36,37]. We therefore performed immunohistochemistry to look for expression of the corresponding proteins/peptides in dorsal root ganglia from 3 mice in each case. We found that 11.9% (9.8-13.8%) of GFP-containing cells were immunoreactive for Vglut3 and 26.4% (22.4-30.9%) for Trpv1 (Figure 1–figure supplement 1A-D). Among the neuropeptides, we found minimal co-localisation with CGRP (mean 2.5%, range 1.4-4.5%) and none with somatostatin. However, 56% (range 55.8-56.3%) of the GFP cells contained

Click here to enter text.

substance P, although this was expressed at relatively low levels (Figure 1–figure supplement 1G-M). These results are therefore consistent with the transcriptomic findings described above[36,37].

Central projections of Trpm8-expressing primary afferents have been shown to terminate mainly in lamina I[20-22], and we found a similar pattern in the spinal cords of Trpm8^{Flp};RCE:FRT mice, with the great majority of GFP-labelled axons remaining in lamina I, and very few passing ventrally (Figure 2). A similar pattern of labelling was observed in all spinal segments examined. We had previously noted that when lamina I was viewed in horizontal sections, Trpm8 afferents were arranged in interweaving bundles that frequently followed the dendrites of a distinctive subset of projection neurons[13]. Consistent with this, we found that Trpm8 afferents labelled with GFP showed a discontinuous arrangement within lamina I when viewed in transverse sections and did not occupy the whole medio-lateral extent of the lamina (Figure 2). The GFP-labelled afferents did not show any obvious restriction in the medio-lateral axis, and could be seen in medial, central and lateral parts of lamina I. Since the great majority of Trpm8-expressing afferents contain GFP in this genetic cross, it is unlikely that the large spaces between bundles of GFP-labelled afferents in lamina I are filled by Trpm8-expressing afferents that lack GFP. This “incomplete” innervation of lamina I by Trpm8 afferents is therefore likely to be genuine.

It has been reported that some lamina I projection neurons were associated with boutons that were immunoreactive for Vglut3[38] and since 12% of Trpm8 afferent cell bodies contained Vglut3, we looked for expression of the transporter in their central terminals. In transverse sections, Vglut3-immunoreactive axons formed a dense band in inner lamina II that corresponds to central terminals of C-low threshold mechanoreceptors (C-LTMRs)[39,40]. However, there were a few Vglut3-immunoreactive boutons in lamina I that were also GFP-positive, indicating that central terminals of some Trpm8-expressing primary afferents had detectable levels of the transporter (Figure 2–figure supplement 1A-F). We generated a mouse genetic cross (Phox2a::Cre;Ai9;Trpm8^{Flp};RCE:FRT) in which a subset of ALS cells express tdTomato and Trpm8 afferents express GFP. In horizontal sections from these mice we identified lamina I projection neurons that were associated with numerous GFP-labelled (Trpm8-expressing) boutons and found that some of these boutons contained Vglut3 (Figure 2–figure supplement 1G-J). The proportion of GFP-labelled boutons that contained Vglut3 varied considerably between cells. Since C-LTMRs do not appear to arborise in lamina I[35], it is likely that the Vglut3-containing boutons that

Click here to enter text.

136 have been found to contact projection neurons in this lamina[38] belong to Trpm8 afferents.
137 Even though many Trpm8-positive cell bodies showed Trpv1 and substance P
138 immunoreactivities, we were not able to detect either of these in their central terminals
139 (Figure 2–figure supplement 1K-M).
140 Although we did not investigate the distribution of GFP in the brains of
141 Trpm8^{Flp};RCE:FRT mice in detail, we noted that there was dense axonal labelling in the
142 spinal trigeminal nucleus, while scattered GFP-labelled cell bodies were present in various
143 brain regions that are known to contain Trpm8-expressing neurons, including the preoptic
144 area and the reticular nucleus of the thalamus[41] (data not shown).
145
146 **Synaptic input from Trpm8-expressing afferents to lamina I projection neurons.**
147 We had previously shown that ~20% of lamina I projection neurons retrogradely
148 labelled from the LPB received numerous contacts from GFP-labelled afferents in
149 Trpm8^{Flp};RCE:FRT mice, and that these contacts were associated with punctate staining
150 for Homer1[13] (a marker for glutamatergic synapses[42]). To reveal synapses formed
151 between Trpm8 afferents and these projection neurons at the ultrastructural level, we used
152 a combined confocal/electron microscopic method[43] on spinal cord tissue from
153 Phox2a::Cre;Ai9;Trpm8^{Flp};RCE:FRT mice. This genetic cross was chosen because we had
154 previously shown that the Phox2a-lineage includes many lamina I ALS neurons with dense
155 input from Trpm8 afferents[13]. Horizontal sections from lumbar spinal cord segments of 2 of
156 these mice were immunostained to reveal tdTomato and GFP, and 3 tdTomato-labelled
157 cells with numerous contacts from GFP-labelled axons were scanned with a confocal
158 microscope (Figure 3, Figure 3–figure supplements 1 and 2). The tissue was subsequently
159 processed with an immunoperoxidase method to label the GFP-positive axons with
160 diaminobenzidine (DAB), and examined with an electron microscope (Figure 3, Figure 3–
161 figure supplement 2). Although the cell bodies and dendrites of the projection neurons did
162 not contain an electron-dense label, they could be readily identified by their location within
163 the ultrathin sections, by their association with numerous DAB-labelled axonal boutons
164 and by the morphology of their somata and proximal dendrites (Figure 3A,B). Because of
165 the very high density of GFP-labelled boutons that were seen to contact the cells in the
166 confocal images, it was not always possible to relate individual boutons from confocal
167 images to those seen with the electron microscope. However, we were able to identify
168 numerous axosomatic and axodendritic synapses (a minimum of 10 synapses per cell)
169 between the GFP-immunoreactive boutons and the lamina I projection neurons. These

Click here to enter text.

170 could be recognised by the presence of darkening of the membranes and in some cases a
171 faint postsynaptic density, together with clustering of synaptic vesicles on the presynaptic
172 side (Figure 3B-D, Figure 3–figure supplement 2C-J). Interestingly, the synapses between
173 the GFP-containing boutons and the projection neurons generally had relatively faint
174 postsynaptic densities and only small regions where the vesicles were clustered on the
175 presynaptic side. These findings, together with our previous observation of Homer1-
176 immunoreactive puncta located between GFP-expressing afferent boutons and the cell
177 bodies and dendrites of retrogradely labelled lamina I projection neurons in
178 Trpm8^{Flp};RCE:FRT mice[13], indicate that ALS cells belonging to this population receive
179 numerous synapses from Trpm8-expressing primary afferents.
180 To provide electrophysiological evidence for synapses between Trpm8 afferents and
181 this population of lamina I ALS cells, we carried out optogenetic experiments. Two
182 Trpm8^{Flp};RCE:FRT mice received intraperitoneal injections of
183 AAV.PHP.S.Flp^{ON}.ChR2_YFP as neonates to label Trpm8-expressing primary afferents
184 with channelrhodopsin. They were then injected with AAV11.tdTomato into the CVLM or
185 LPB ~5 weeks later (Figure 3E). Whole-cell patch-clamp recordings were subsequently
186 obtained from tdTomato-labelled lamina I neurons in a whole-cord preparation. We used
187 the Trpm8^{Flp};RCE:FRT cross for these experiments in order to allow un-biased
188 identification of ALS neurons that were surrounded by Trpm8 afferents. Importantly,
189 although the viral delivery approach that we used will have specifically targeted Trpm8
190 afferents, it will not have resulted in adequate expression of channelrhodopsin in all of
191 these cells.
192 We identified 8 tdTomato cells that were densely surrounded by GFP-labelled (Trpm8)
193 afferents and found that 1 ms blue light pulses induced EPSCs in 5 of these cells (Figure
194 3E,F). We measured the latency of the first EPSC after blue light pulses (0.2 Hz) and
195 found that the latency jitter was less than 1 ms, indicating that these neurons receive
196 monosynaptic inputs[44] (Figure 3F; n = 5, Average latency: 5.8 ± 0.86 ms, latency jitter:
197 0.68 ± 0.14 ms). Two of the 5 neurons showed multiple peaks with a larger latency jitter,
198 indicating that there may also have been polysynaptic inputs (Figure 3–figure supplement
199 3). It is likely that the remaining 3 cells received input from Trpm8 afferents that did not
200 express sufficiently high levels of channelrhodopsin. Together, these findings demonstrate
201 that Trpm8 afferents directly synapse onto lamina I ALS cells that are surrounded by these
202 afferents.
203

Click here to enter text.

204 **Lamina I ALS neurons that are surrounded by Trpm8 afferents are cold-selective**

205 We next tested whether the lamina I projection neurons that are densely innervated by
206 Trpm8 afferents correspond to the cold-selective neurons identified in physiological
207 studies[23-33]. To do this, we carried out whole-cell patch-clamp recordings in preparations in
208 which ALS neurons were retrogradely labelled with either mCherry or tdTomato, and
209 Trpm8 axons expressed GFP. Retrograde labelling was achieved by injecting
210 AAV9.mCherry into the CVLM or LPB of Trpm8^{Flp};RCE:FRT mice, resulting in mCherry
211 labelling, or else by injecting AAV9.Cre_GFP into the CVLM of Trpm8^{Flp};RCE:FRT;Ai9
212 mice leading to tdTomato labelling (Figure 4A). We used the semi-intact *ex vivo*
213 somatosensory preparation, in which the spinal cord, L2 and L3 roots and ganglia,
214 saphenous and femoral cutaneous nerves, and hindlimb skin are dissected in continuity
215 (Fig 4B)[31,32].

216 Visualisation of the spinal cord with filter sets for GFP or mCherry/tdTomato revealed
217 lamina I projection neurons (labelled with mCherry or tdTomato) as well as a plexus of
218 GFP-labelled (Trpm8-expressing) primary afferents (Figure 4). We recorded from 6
219 mCherry/tdTomato-labeled projection neurons that had dendrites (and in some cases also
220 cell bodies) that were clearly associated with numerous GFP-labelled afferents, as well as
221 from 5 projection neurons for which there was no clear association with these afferents.
222 We assessed the responses of these cells to a 4 g von Frey filament, hot saline (50°C),
223 and cold saline (15°C) applied to the skin[31]. All 6 of the projection neurons that had
224 numerous contacts from GFP-labelled axons responded exclusively to application of cold
225 saline. In 4 cases recordings were made in current clamp and the cells fired action
226 potentials (n = 3) or generated EPSPs (subthreshold, n = 1) following application of cold
227 saline, but showed no response to mechanical or heat stimuli (Figure 4C-E). The time
228 course of the response was consistent with that seen for cold-selective projection neurons
229 that we previously reported (Figure 4–figure supplement 1)[32]. The other two cells with
230 numerous GFP contacts were recorded in voltage clamp, and these showed EPSCs in
231 response to cold, but not mechanical or heat, stimuli. All six of these neurons were
232 therefore classified as cold-selective. The five projection neurons that were not
233 preferentially associated with GFP-labelled afferents were all recorded in current clamp
234 mode, and all of these cells exhibited action potential firing in response to mechanical
235 stimulation. Three of them also responded to heat, and one additionally to cold stimuli. The
236 five neurons that were not associated with numerous GFP-labelled afferents were
237 therefore classified as either mechano-selective or polymodal (Figure 4F-H).

Click here to enter text.

238 We previously reported that cold-selective projection neurons are distinct from other
239 lamina I projection neurons[32], and a defining feature of these cells was their low frequency
240 of spontaneous EPSCs (sEPSCs). We therefore quantified sEPSC frequency and
241 amplitude in lamina I projection neurons with or without dense Trpm8 input. As expected,
242 neurons with dense Trpm8 input had significantly lower sEPSC frequencies compared to
243 those that lacked dense Trpm8 input (Figure 4–figure supplement 1). Interestingly, the
244 amplitude of sEPSCs in the projection neurons with dense Trpm8 input was smaller than
245 in those that lacked this input, which had not been observed in our previous study[32].
246 Together, these results strongly suggest that lamina I projection neurons receiving dense
247 Trpm8 afferent innervation constitute a distinct neuronal population specialised for cold
248 sensation, and correspond to the cold-selective ALS neurons identified in previous
249 studies[23-33].
250 Our anatomical studies indicate that the cells densely coated with Trpm8-expressing
251 primary afferents receive many synapses from these afferents (Figure 3), and we had
252 shown previously that these cells had numerous Homer1-immunoreactive puncta, with
253 ~60% being associated with a Trpm8-expressing primary afferent bouton[13]. The low
254 frequency of sEPSCs is therefore not likely to result from a low density of synapses, but
255 presumably reflects a very low release probability at these synapses in these experimental
256 conditions. The lower amplitude of sEPSCs may be related to our EM observation that
257 contacts between Trpm8 afferents and densely coated lamina I projection neurons
258 typically have small synaptic specialisations (Figure 3, Figure 3–figure supplement 2).
259
260 **Targeting of cold-selective lamina I ALS neurons with the Calb1^{Cre} mouse**
261 We had previously demonstrated that lamina I projection neurons that are densely
262 innervated by Trpm8-expressing afferents are included among those of the Phox2a-
263 lineage, and contain mRNA for *Hs3st1*, one of the top differentially expressed genes for
264 ALS3. We had therefore assigned the Trpm8-innervated cells to the ALS3 cluster[13]. Calb1,
265 which encodes the calcium-binding protein calbindin, is also among the top 20 differentially
266 expressed genes for ALS3 (Figure 5–figure supplement 1A, see also Figure 1D of
267 reference[13]). However, calbindin is not restricted to the ALS3 cluster, as it is also
268 expressed by some cells in the ALS2, ALS4 and ALS5 clusters[13] (Figure 5–figure
269 supplement 1A), and by many ALS neurons in the lateral spinal nucleus (LSN)[45], most of
270 which are not derived from the Phox2a-lineage[14,46].

To assess the relationship between Calb1-expressing ALS neurons and those with dense Trpm8 innervation, we injected an AAV coding for Cre-dependent tdTomato (AAV11.Cre^{ON}.tdTomato[47]) unilaterally into the LPB of 4 Calb1^{Cre};Trpm8^{Flp};RCE:FRT mice (Figure 5–figure supplement 1B). As expected from the known distribution of calbindin-expressing ALS cells in the rat[45], we observed tdTomato-positive cells in lamina I (mainly on the contralateral side), as well as bilaterally in the LSN and in deeper laminae (Figure 5A, Figure 5–figure supplement 1C-F). When we examined horizontal sections through lamina I, we found that many of the tdTomato-labelled cells, were densely innervated by Trpm8 afferents (Figure 5C-H), and these were located throughout the mediolateral extent of the dorsal horn. The proportion of tdTomato cells with dense Trpm8 input varied between 38.7-59.6% across the L2-L4 segments (Figure 5B, RM ANOVA, $p = 0.048$). Interestingly, the proportion was significantly higher in L2 (59.6%) than in L4 (38.7%), (RM ANOVA, Holm-Šídák's multiple comparisons test, $p = 0.0056$, $n = 4$), and this may reflect a difference in the proportion of lamina I cells with dense Trpm8 innervation between segments. When results across the 3 segments were pooled, the total numbers of retrogradely labelled cells ranged from 133 to 170 (mean 151), while the proportions with dense Trpm8 input ranged from 46.5%-54.1% (mean 50.6%). To confirm expression of calbindin in lamina I projection neurons with dense Trpm8 input, we carried out immunofluorescence labelling on horizontal sections from 3 Trpm8^{Flp};RCE:FRT mice that had received injections of AAV9.mCherry into the LPB. We identified a total of 32 mCherry-positive lamina I neurons that were associated with dense GFP labelling (6-14 per mouse), and found that all but four of these (27/31, 87%) were calbindin-immunoreactive (Figure 5–figure supplement 1G).

We also used the semi-intact preparation to record from tdTomato-labelled lamina I neurons in spinal cords from 4 Calb1^{Cre} mice that had received injections of AAV11.Cre^{ON}.tdTomato into the CVLM (Figure 5–figure supplement 1B, Figure 5–figure supplement 2). We recorded from 6 retrogradely labelled neurons and found that 5 were cold-selective, while one was polymodal, responding to brushing of the skin, as well as to application of both hot and cold stimuli (Figure 5I,J). These cold-selective neurons showed a similar time course in response to cold stimulation to those described above (Figure 5–figure supplement 2C). Taken together, these findings indicate that while Calb1 is not restricted to cold-selective cells, many of the Calb1-expressing projection neurons in lamina I belong to the cold-selective population.

Click here to enter text.

305 **Brain projections of putative cold-selective lamina I neurons**

306 Because Calb1 is expressed by cold-selective ALS cells in lamina I, we carried out
307 anterograde tracing by injecting AAV coding for Cre-dependent expression of tdTomato
308 (AAV1.Cre^{ON}.tdTom) into the lumbar spinal cords of Calb1^{Cre} mice. Our aim was to test for
309 projections to two potential brainstem targets that receive input from the ALS[11,12] and also
310 contain many neurons that express the immediate early gene Fos in mice exposed to low
311 ambient temperatures[48-51]: the caudal part of the PAG (cPAG), and the rostral part of the
312 LPB, in particular a region that has been named PBrel (rostral to external lateral)[49]. Two
313 cortical areas are activated by skin cooling, the primary somatosensory and posterior
314 insular cortices[52]. We therefore looked for evidence of an input to the ventral posterolateral
315 (VPL) and posterior triangular (PoT) thalamic nuclei, which are thought to provide the
316 thermosensory inputs to these cortical areas in rodents[53]. Initially, we examined labelling
317 resulting from injections of AAV1.Cre^{ON}.tdTomato that were targeted on the central part of
318 the dorsal horn, either in the L3 segment, or in the L3, L4 and L5 segments, using a similar
319 approach to that which we had taken with other genotypes (Figure 6–figure supplement
320 1A,B; Table 1). Labelling patterns were consistent among the mice used in this part of the
321 study, but labelling was denser in all regions in those that had received injections into L3,
322 L4 and L5. This approach revealed that axons ascended in the dorsolateral white matter of
323 the spinal cord and gave branches to several regions on the contralateral side of the
324 brainstem, including LPB and the cPAG (Figure 6–figure supplement 1C,D). Within the
325 LPB, axonal labelling was very dense in the rostral-most part, which corresponds to
326 PBrel[49], and moderately dense in the centrolateral (PBcl) nucleus. In addition, there was
327 some labelling in other nuclei, including external lateral (PBel), dorsolateral (PBdl) and
328 internal lateral (PBil). There was dense labelling in the cPAG and in addition, labelling was
329 seen within the superior colliculus (Figure 6–figure supplement 1C). In the thalamus, there
330 was sparse labelling in the VPL, posterior (Po) and PoT nuclei contralateral to the injection
331 site, and many labelled profiles were present in the medial thalamus on both sides (Figure
332 6–figure supplement 1E). These findings were therefore consistent with the expected
333 projections of cold-selective ALS cells to PBrel, cPAG and the VPL nucleus of thalamus.

334 However, this strategy will also have labelled Calb1-expressing projection neurons in
335 other regions, including the LSN and the lateral reticulated part of lamina V (Figure 6–
336 figure supplement 1B). Consistent with this interpretation, we observed labelling in PBil
337 and the medial thalamus, both of which are known to receive input from ALS cells in the
338 deep dorsal horn[54-56], including cells belonging to the ALS4 population in lateral lamina V[5].

Click here to enter text.

339 We therefore altered the injection technique by reducing the volume and injecting at a
340 more medial location (250 μm rather than 400 μm lateral to the midline). As with the
341 previous experiments, these injections were either made into the L3 segment, or into each
342 of L3, L4 and L5 (Table 1). Again, the pattern of labelling was consistent among these
343 mice, but labelling was denser in those that had received injections into L3, L4 and L5.
344 This strategy resulted in injection sites that were restricted to the medial part of the dorsal
345 horn and excluded the LSN (Fig 6A-C). Although very weak tdTomato labelling was seen
346 in the LSN in these experiments, this is likely to have arisen from transport by axons of
347 local calbindin-expressing excitatory interneurons, since many excitatory interneurons in
348 laminae I-II have axons that enter the LSN[57-59]. Importantly, no tdTomato-labelled cell
349 bodies were seen in the LSN or in the lateral reticulated part of lamina V in these cases.
350 Since these injections were likely to have included a much higher proportion of lamina I
351 neurons with dense Trpm8 innervation, we analysed the anterograde labelling in more
352 detail.
353 Axons ascended in the dorsal quadrant of the spinal cord, mainly on the contralateral
354 side (Figure 6–figure supplement 2A). Although a few collaterals arose at all segmental
355 levels examined, these were far less numerous than those originating from the
356 somatostatin-expressing ALS cells that occupy the lateral part of lamina V[5]. Ascending
357 axons lay near the ventrolateral surface of the medulla, and sent collateral branches to the
358 NTS (Figure 6D), but unlike Gpr83- and Tacr1-expressing ALS cells[5,60], these Calb1-
359 positive cells did not innervate the inferior olive. Labelling in the LPB was much more
360 restricted following medial spinal injections, compared to the central injections (Figure 6E,
361 Figure 6–figure supplement 1C,D, Figure 6–figure supplement 2B). In particular, labelling
362 in PBcl and PBil was greatly reduced, while the dense input to the PBrel was retained. The
363 input to PBrel was confirmed by immunostaining for the transcription factor Foxp2, which is
364 expressed in PBrel neurons (Fig 6G,H)[49]. There was also strong labelling in the lateral part
365 of the cPAG, (Figure 6E), but only very sparse labelling in the rostral part of the PAG
366 (Figure 6–figure supplement 2C,E). Input to both LPB and PAG was bilateral, but denser
367 on the side contralateral to the spinal injections. Labelling in the superior colliculus was
368 almost completely lost following medial spinal injections (Figure 6E). Within the thalamus,
369 the sparse labelling in VPL and Po was still present, but that in the medial thalamus was
370 far weaker (Figure 6F,I,J). In addition, medial spinal injections resulted in labelling in the
371 PoT nucleus of the thalamus (Figure 6–figure supplement 2C,D), which is a known target
372 for lamina I ALS neurons[56,61] and is thought to convey non-noxious thermal information to

Click here to enter text.

373 the posterior insular cortex[53]. Very few, if any, tdTomato-labelled axons were seen in any
374 other parts of the diencephalon[62]. High magnification scans showed that in the regions
375 targeted by tdTomato labelled axons (NTS, LPB, PAG, thalamus) these axons possessed
376 numerous varicosities, which presumably correspond to axonal boutons (Figure 6–figure
377 supplement 2F). Immunostaining for the postsynaptic density protein Homer1 revealed
378 that varicosities were often apposed to Homer1 puncta (Figure 6–figure supplement
379 2G,H), confirming that they constituted the presynaptic elements at glutamatergic
380 synapses.

381 We have previously demonstrated that although spinothalamic lamina I neurons are
382 relatively common in the rodent cervical enlargement, they are far less numerous at
383 lumbar levels, accounting for <5% of lamina I ALS neurons[46,63]. We therefore injected
384 AAV1.Cre^{ON}.tdTom into the cervical enlargement of 3 Calb1^{Cre} mice (Table 1, Figure 6–
385 figure supplement 3A,B). This resulted in far denser axonal labelling within the VPL and
386 PoT nuclei on the side contralateral to the spinal injection (Figure 6–figure supplement 3C-
387 E).

388 The differences between projection patterns of medial and central injections into the
389 lumbar enlargement provide additional information about potential targets of Calb1 cells
390 that were not located in lamina I. As noted above, the input to PBil and medial thalamus
391 seen following the central injections is likely to result at least in part from capture of cells
392 belonging to the ALS4 population in lateral lamina V[13], since we have shown that these
393 cells (targeted in a Sst^{Cre} mouse line) project to these two sites[5]. However, we found only
394 very sparse input from the Sst-expressing (ALS4) cells to the superior colliculus[5], raising
395 the possibility that input to the colliculus originates mainly from cells in the LSN, many of
396 which express Calb1. Consistent with this suggestion, Choi et al[60] observed a projection to
397 the superior colliculus from Tacr1-expressing ALS cells, and many ALS neurons in the
398 LSN express the neurokinin 1 receptor (NK1r), which is encoded by Tacr1[64-66].

399 To confirm the input to PAG from cold-selective lamina I cells, we targeted injections of
400 AAV11.Cre^{ON}.tdTomato to the caudal PAG in 3 Calb1^{Cre};Trpm8^{Flp};RCE:FRT mice. In these
401 experiments, the total numbers of retrogradely labelled (tdTomato-positive) lamina I cells
402 in the L2-L4 segments were lower than was the case for the LPB injection experiments
403 (26, 59 and 99 in the three cases), but the proportion of these cells that had dense Trpm8
404 input was significantly higher: 84.6%, 81.4% and 77.8% ($p < 0.0001$, unpaired t-test with
405 Welch's correction; Figure 6–figure supplement 4). This indicates that, at least for

406 calbindin-expressing lamina I ALS neurons, cold-selective cells are highly enriched among
407 those that project to the caudal part of the PAG.
408 Finally, we looked for further evidence of a projection from cold-selective lamina I cells
409 to the lateral part of the thalamus by making small injections of cholera toxin B subunit
410 (CTB) in 3 Trpm8^{Flp};RCE:FRT mice. CTB was used as a retrograde tracer for these
411 experiments, because it can result in relatively small and well-defined injection sites. In all
412 3 cases, the injection was centred on the ventral posterior nucleus of thalamus, and
413 included both lateral (VPL) and medial (VPM) parts (Figure 6–figure supplement 5A-C).
414 There was some spread into Po and the ventrolateral (VL) nucleus, but none into the
415 medial thalamus and none of the injections extended as far caudally as the PoT. As
416 expected, from the low number of lamina I spinothalamic neurons at lumbar levels[46,63], few
417 (if any) retrogradely labelled cells were seen in the lumbar spinal cord in these
418 experiments (5 cells in the L4 segment of one mouse, but no cells in this segment in the
419 other two), and for this reason we focused our search on the cervical enlargement. In
420 horizontal sections through the C7 segment, we identified a large number of retrogradely
421 labelled lamina I cells in each case. Although the dendritic filling was less complete than
422 that seen with retrograde viral tracing, we were able to identify many CTB-positive cells
423 that received numerous contacts on cell bodies and dendrites from Trpm8-expressing
424 primary afferents (Figure 6–figure supplement 5D-I). In the one case in which retrogradely
425 labelled cells were detected in the L4 segment, 3 of the 5 cells were also densely coated
426 with GFP-labelled afferents (Figure 6–figure supplement 5J-L). These findings
427 demonstrate that cold-selective lamina I ALS neurons project to the lateral thalamus.
428
429 **DISCUSSION**
430 The main findings of this study are that: (1) lamina I projection neurons that are densely
431 innervated by Trpm8-expressing primary afferents correspond to the cold-selective cells
432 identified in physiological studies and receive monosynaptic input from Trpm8 afferents;
433 (2) these are captured when AAVs encoding Cre-dependent constructs are injected into
434 the brains of Calb1^{Cre} mice; and (3) axons of Calb1-positive neurons in the medial part of
435 the dorsal horn project to brain regions known to be involved in processing information
436 related to cold input, PBrel, caudal PAG, as well as the PoT and VPL nuclei of the
437 thalamus. This suggests that these sites are directly innervated by cold-selective ALS
438 neurons in lamina I.
439

440 **Lamina I ALS neurons with dense Trpm8 input are cold-selective**

441 We had previously observed that Trpm8-expressing primary afferents are closely
442 associated with the cell bodies and dendrites of a subset of ALS cells in lamina I[13]. Based
443 on their association with Homer1 puncta, we were also able to estimate that GFP-labelled
444 (Trpm8-expressing) afferents accounted for ~60% of the excitatory synapses on these
445 ALS cells. Here we directly demonstrate the presence of synapses with both electron
446 microscopy and optogenetics, and confirm our prediction[13] that these densely Trpm8-
447 innervated ALS cells correspond to the cold-selective neurons identified in previous
448 physiological studies[23-33].

449 Cold-selective lamina I projection neurons have been reported in several species,
450 including monkey[27], cat[23-26], rat[28,30] and mouse[29,31-33], and a recent *in vivo* calcium-imaging
451 study reported that they accounted for ~15% of lamina I spinoparabrachial neurons in the
452 mouse[33]. Although cold-selective lamina I projection neurons respond predominantly to
453 skin cooling, some show a weak "paradoxical" response when noxious heat is applied to
454 the skin[24,26,27,29]. We did not detect any response from cold-selective cells when hot saline
455 was applied to the skin in the experiments reported here, or in our previous study of cold-
456 selective neurons[32], and this may be because although the temperature of the hot saline
457 was 50°C, the small volume applied to the skin meant that skin temperature did not reach
458 a sufficiently high level to result in activation. It is known that some Trpm8-expressing
459 primary afferents have low levels of Trpv1[20,35,37], and some Trpm8 afferents have been
460 shown to respond weakly to noxious heat *in vivo*[35]. It has been proposed that there are two
461 different populations of Trpm8-expressing afferents: one consisting of cells that lack Trpv1
462 and respond to innocuous cooling, and the other of cells that express Trpv1, and may
463 function as "cold nociceptors"[67]. Since we found Trpv1-immunoreactivity in around a
464 quarter of GFP-labelled dorsal root ganglion cells, it is likely that both populations are
465 included amongst the GFP-expressing cells in the Trpm8^{Flp};RCE:FRT mice. However, we
466 were unable to detect Trpv1-immunoreactivity in the central terminals of any GFP-positive
467 axons (presumably reflecting the low level of Trpv1 expressed by these cells), and we
468 therefore do not know whether the Trpm8-positive axons synapsing on cold-selective
469 lamina I ALS neurons include those that express Trpv1. However, if this is the case, it is
470 likely to explain the weak response to noxious heat reported for some cold-selective
471 projection neurons[24,26,27,29].

472

Click here to enter text.

473 **Direct and indirect input from Trpm8 afferents to cold-selective ALS neurons**

474 Our findings clearly demonstrate a major direct (monosynaptic) input from Trpm8-
475 expressing primary afferents to cold-selective lamina I projection neurons. We had
476 previously estimated that a mean of 62% of the Homer1 puncta (which correspond to
477 excitatory synapses) on cell bodies and dendrites of these cells were associated with
478 GFP-positive boutons in Trpm8^{Flp}:RCE:FRT mice[13]. However, we show here that this line
479 only labels ~83% of Trpm8-expressing primary afferent neurons with GFP. If this
480 proportion applies equally to Trpm8 afferents that synapse on cold-selective ALS cells,
481 then Trpm8 afferents would give rise to ~75% of the excitatory synapses on these cells.

482 Lee et al[34] recently proposed that there is a dedicated population of superficial dorsal
483 horn excitatory interneurons that express the thyrotropin releasing hormone receptor (Trhr)
484 and form a disynaptic link between Trpm8 afferents and cold-selective lamina I projection
485 neurons. Interestingly, in their initial experiments, they ablated or silenced calbindin-
486 expressing dorsal horn neurons and found that this reduced behavioural responses to skin
487 cooling. Although they interpreted this as resulting from loss of function of calbindin-
488 expressing excitatory interneurons, our findings indicate that they are also likely to have
489 ablated or silenced calbindin-expressing cold-selective lamina I ALS neurons. This could
490 therefore have made a major contribution to the reduced sensitivity to skin cooling. Having
491 obtained evidence that cold-responsive Calb1+ neurons in the dorsal horn often co-
492 expressed Trhr, Lee et al generated a Trhr^{Cre} mouse line and used spinal injection of AAVs
493 coding for Cre-dependent constructs, or a genetic intersectional approach, to target Trhr-
494 expressing spinal neurons[34]. They ablated these cells and found that this selectively
495 reduced responses to skin cooling. They also reported that when AAV.Cre^{ON}.YFP was
496 injected intraspinally in Trhr^{Cre} mice, there was no axonal labelling in the brain, suggesting
497 that Trhr-expressing dorsal horn neurons were exclusively interneurons. However, this
498 observation is not consistent with our transcriptomic dataset[13], which reveals Trhr
499 expression in some Phox2a-derived ALS neurons, including some of those in the ALS3
500 cluster (Figure 7-figure supplement 1). It is therefore not clear why a brain projection from
501 Trhr cells was not detected by Lee et al, although it is possible that the survival time
502 allowed for anterograde transport of YFP (reported as 2-3 weeks) was not sufficient. Lee
503 et al[34] also reported that the cold-selective ALS neurons were marked by expression of the
504 calcitonin receptor-like receptor (encoded by the *Calcrl* gene). However, this is unlikely to
505 be a specific marker, as our data show expression of Calcrl among several populations of
506 Phox2a-derived ALS neurons[13] (Figure 7-figure supplement 1), and it has been reported

Click here to enter text.

507 that Calcrl is also expressed by spinoparabrachial neurons that are required for
508 mechanical itch[68].
509 While our findings do not exclude the possibility that there is a specific population of
510 interneurons that link Trpm8-expressing primary afferents to cold-selective ALS neurons in
511 lamina I, they clearly demonstrate a substantial direct (monosynaptic) input from Trpm8
512 afferents to cold-selective lamina I projection neurons, and indicate the need for caution in
513 relying on the specificity of individual genetic markers to define neurons and circuits in the
514 dorsal horn.
515
516 **Brain targets of cold-selective ALS cells**
517 At present there is no known molecular marker that could be used to target cold-
518 selective lamina I ALS cells exclusively. We chose calbindin because *Calb1* is among the
519 top differentially expressed genes in the ALS3 cluster[13], and there is a well-established
520 knock-in Cre line available[69]. Importantly, our transcriptomic analysis[13] was restricted to
521 projection neurons derived from the Phox2a lineage[14], which excludes most ALS cells in
522 the LSN and ~40% of those in lamina I[14,46]. Menetrey et al[45] had demonstrated that
523 calbindin-immunoreactive spinoparabrachial neurons in rat were located in lamina I, the
524 LSN and lateral lamina V, with scattered cells around the central canal, and this closely
525 matches the distribution of cells labelled when AAV11.Cre^{ON}.tdTomato was injected into
526 the LPB of Calb1^{Cre} mice. For anterograde tracing, we were able to exclude LSN and
527 lateral lamina V ALS cells by injecting smaller volumes into the medial part of the dorsal
528 horn, and this was confirmed by the lack of axonal labelling in regions known to receive
529 input from these cells (e.g., PBil and medial thalamus)[5,54,56]. However, although our medial
530 injections preferentially captured cold-selective lamina I ALS neurons they will also have
531 labelled cells that are not cold-selective, including some lamina I cells in the ALS2 cluster[13]
532 and potentially some of those that are not derived from the Phox2a lineage[46]. We therefore
533 focused our analysis on brain regions known to be involved in cold sensing, and tested
534 whether these received input from the Calb1-positive ALS cells.
535 Among the ALS projection targets that contain cells responding to cold, we were able to
536 show a dense input to the rostral part of the LPB and to the cPAG. Two studies have
537 mapped neurons in LPB that express Fos in mice exposed to low ambient
538 temperatures[49,50], and both found that Fos-positive cells were concentrated in the rostral
539 part of the LPB, corresponding to a level ~4.9 mm caudal to bregma (or 1.1 mm caudal to
540 the interaural line)[62]. Yang et al[50] identified the region containing Fos+ cells as part of the

Click here to enter text.

541 external lateral (PBel) nucleus, while Geerling et al[49] defined it as the PBrel, and showed
542 that this area could be recognised by the expression of Foxp2. Yang et al[50] reported that
543 cold-activated cells in this region projected to the preoptic area (POA), which is known to
544 form part of a cold-defence circuit[70], as well as to the dorsomedial hypothalamus (DMH).
545 They also showed that parabrachial neurons targeting DMH promoted activation of brown
546 adipose tissue, suggesting a role for both of these hypothalamic areas in maintenance of
547 body temperature in cold conditions. The cold-selective lamina I ALS cells are therefore
548 likely to provide an important source of input to POA and DMH via their projection to PBrel,
549 thus forming part of the afferent limb of a cold defence pathway (Figure 7).
550 Neurons in the cPAG show increased Fos expression in rats exposed to low ambient
551 temperatures[48], and this region receives an input from cold-activated cells in the
552 hypothalamus[51]. Our results demonstrate that Calb1-positive neurons in the dorsal horn
553 also provide a dense input to the cPAG. Although we cannot be certain that this originates
554 from the cold-selective ALS neurons, there are two lines of evidence to support this
555 suggestion. First, Li et al[71] demonstrated innervation of mouse lamina I spino-PAG
556 neurons by Trpm8-expressing primary afferents, and second, we found that ~80% of
557 Calb1 neurons retrogradely labelled from cPAG received dense Trpm8 input. Consistent
558 with this interpretation, we had previously reported that rat lamina I neurons retrogradely
559 labelled from the PAG seldom showed strong expression of the NK1r, unlike those labelled
560 from the LPB or CVLM[72], and cold-selective lamina I neurons have been shown to respond
561 weakly, if at all, to substance P, the main ligand for this receptor[32]. These findings suggest
562 that the cold-selective lamina I neurons provide a direct input to cPAG, which presumably
563 contributes to the responsiveness of neurons in this region to cooling[48]. Activation of
564 neurons in the cPAG results in brown adipose tissue thermogenesis[73], suggesting a role in
565 maintenance of body temperature in cold conditions (Figure 7).
566 Our CTB injections into the lateral thalamus were centred on the ventral posterior
567 nucleus, with a varying degree of spread into Po, which was also found to receive input
568 from Calb1-positive ALS neurons. It is not possible to determine precisely the region(s)
569 from which retrograde transport would occur, but since we identified lamina I cells in the
570 C7 segment (and in one case also in the L4 segment) with relatively strong CTB labelling
571 that were associated with GFP-labelled axons, these are likely to have projected to the
572 core of the injection site, i.e. the ventral posterior nucleus. As noted above, spinothalamic
573 lamina I neurons are infrequent in the rodent lumbar enlargement[46,63], and this presumably
574 accounts for the very sparse labelling in VPL that we saw following injections of

Click here to enter text.

575 AAV1.Cre^{ON}.tdTomato into the lumbar spinal cord, compared to that seen after cervical
576 injections. However, our findings from the retrograde tracing experiments suggest that
577 cold-selective cells project to VPL, and this is consistent with the demonstration of input
578 from cervical lamina I neurons to VPL in the rat[56]. In addtion, we identified an input to the
579 PoT nucleus of thalamus, which projects to the posterior insular cortex[53]. Together, the
580 input from cold-selective lamina I ALS cells to PoT and VPL is likely to contribute to the
581 perception of cold stimuli applied to the skin through the projections of these thalamic
582 nuclei to the posterior insular and somatosensory cortices[53] (Figure 7).
583
584
585 **MATERIALS AND METHODS**
586
587 **Key resources table**

Reagent or resource	Source	Identifier
Mouse lines		
Trpm8^{Flp}	Dr Mark Hoon	N/A
B6.Cg-Gt(ROSA)26Sor$^{tm9(CAG\text{-}tdTomato)Hze}$/J (Ai9)	Prof. Hongkui Zheng; available from The Jackson Laboratory, ME, USA	Cat#: 007909 RRID: IMSR_JAX:007909
Phox2a::Cre	Prof Artur Kania	N/A
STOCK *Gt(ROSA)26Sor$^{tm1.2(CAG\text{-}EGFP)Fsh}$*/Mmjax (RCE:FRT)	The Jackson Laboratory, ME, USA	Cat#: 032038 RRID:MMRRC_032038-JAX
B6;129S-*Calb1$^{tm2.1(cre)Hze}$*/J (Calb1^{Cre})	The Jackson Laboratory, ME, USA	Cat#: 028532 RRID:IMSR_JAX:028532
AAV constructs		
pENN.AAV.CB7.CI.mCherry.WPRE.RBG (AAV9.mCherry)	Penn Vector Core, PA, USA; available from Addgene, MA, USA	Cat#: 105544-AAV9 RRID:Addgene_105544
pssAAV-2-CAG-EGFP_Cre-WPRE-SV40p(A) (AAV9.EGFP_Cre)	Viral Vector Facility, University of Zurich, Switzerland	Cat#: v25-9
pssAAV-2-CAG-dlox-tdTomato(rev)-dlox-WPRE-bGHp(A) (AAV1.Cre^{ON}.tdTomato)	Viral Vector Facility, University of Zurich, Switzerland	Cat#: v167-1
AAV11.CAG.Cre^{ON}.tdTomato (AAV11.Cre^{ON}.tdTomato)	BrainCase Biotechnology Co Ltd, Wuhan, China	Cat#: BC-0870
AAV.PHP.S.Flp^{ON}.ChR2_YFP	Viral Vector Facility, University of Zurich, Switzerland	Cat#: v237-PHP.S
AAV11.CAG.tdTomato (AAV11.tdTomato)	BrainCase Biotechnology Co Ltd, Wuhan, China	Cat#: BC-0868
Antibodies		
Chicken anti-GFP (1:1000)	Abcam plc	Cat#: ab13970 RRID: AB_300798
Rabbit anti-GFP (1:1000)	M Watanabe	RRID:AB_2571573

Click here to enter text.

Rat anti-mCherry (1:1000)	Thermo Fisher Scientific	Cat#: M11217 RRID: AB_2536611
Guinea pig anti-NeuN (1:1000)	Synaptic Systems	Cat#: 266 004 RRID:AB_2619988
Rabbit anti-NeuN-Alexa Fluor® 647 (1:1000)	Abcam plc	Cat#: EPR12763 RRID:AB_2532109
Rat anti-substance P (1:200)	Oxford biotechnology	Cat#: OBT06435
Rabbit anti-substance P (1:1000)	Peninsula	Cat#: T-4107 RRID:AB_518630
Rabbit anti-TRPV1 (1:1000)	Synaptic Systems	Cat#: 444 013 RRID:AB_2864792
Sheep anti-CGRP (1:2000)	Enzo	Cat#: BML-CA1137 RRID:AB_2243859
Rabbit anti-somatostatin (1:500)	Peninsula	Cat#: T-4103 RRID:AB_518614
Guinea pig anti-VGLUT3 (1:100)	M Watanabe	RRID:AB_2571856
Sheep anti-Foxp2 (1:500)	Biotechne	Cat#: AF5647 RRID:AB_2107133
Goat anti-cholera toxin B subunit (1:2000 for immunofluorescence; 1:100,000 for immunoperoxidase)	List Biological	Cat#: 703 RRID:AB_10013220
Goat anti-Homer1 (1:500)	M Watanabe	RRID:AB_2631104
Rabbit anti-calbindin (1:1000)	Swant	Cat#: CB38 RRID:AB_10000340
Alexa Fluor™ Plus 405 Donkey anti-Rabbit IgG (1:500)	Thermo-Fisher Scientific	Cat#: A48258 RRID: AB_2890547
Alexa Fluor® 488 Donkey Anti-Chicken IgY (1:500)	Jackson ImmunoResearch	Cat#: 703-545-155 RRID: AB_2340375
Alexa Fluor® 488 Donkey anti-Goat IgG (1:500)	Jackson ImmunoResearch	Cat#: 705-545-147 RRID: AB_2336933
Alexa Fluor® 488 Donkey Anti-Rabbit IgG (1:500)	Jackson ImmunoResearch	Cat#: 711-545-152 RRID: AB_2313584
Alexa Fluor™ Plus 488 Donkey anti-Rabbit IgG (1:500)	Thermo-Fisher Scientific	Cat#: A32790 RRID: AB_2762833
Rhodamine Red™-X Donkey Anti-Guinea pig IgG (1:100)	Jackson ImmunoResearch	Cat#: 706-295-148 RRID: AB_2340468
Rhodamine Red™-X Donkey Anti-Rabbit IgG (1:100)	Jackson ImmunoResearch	Cat#: 711-295-152 RRID: AB_2340613
Rhodamine Red™-X Donkey Anti-Rat IgG (1:100)	Jackson ImmunoResearch	Cat#: 712-295-153 RRID: AB_2340676
Alexa Fluor™ Plus 555 Donkey anti-Rat IgG (1:500)	Thermo-Fisher Scientific	Cat#: A48270 RRID:AB_2896336
Alexa Fluor™ Plus 555 Donkey anti-Goat IgG (1:500)	Thermo-Fisher Scientific	Cat#: A32816 RRID:AB_2762839
Alexa Fluor® 647 Donkey Anti-Rabbit IgG (1:500)	Jackson ImmunoResearch	Cat#: 711-605-152 RRID:AB_2492288
Alexa Fluor® 647 Donkey Anti-Goat IgG (1:500)	Jackson ImmunoResearch	Cat#: 705-605-147 RRID: AB_2340437
Alexa Fluor® 647 Donkey Anti-Guinea pig IgG (1:500)	Jackson ImmunoResearch	Cat#: 706-605-148 RRID: AB_2340476

Click here to enter text.

Biotin-SP Donkey Anti-Goat IgG (1:500)	Jackson ImmunoResearch	Cat#: 705-065-147 RRID: AB_2340397
Biotin-SP Donkey Anti-Guinea pig IgG (1:500)	Jackson ImmunoResearch	Cat#: 706-065-148 RRID: AB_2340451
Biotin-SP Donkey Anti-Rabbit IgG (1:500)	Jackson ImmunoResearch	Cat#: 711-065-152 RRID: AB_2340593
Avidin conjugates		
Extravidin-Peroxidase	Sigma-Aldrich	Cat#: E2886 RRID:AB_2620165
Streptavidin-Pacific Blue	Life Technologies	Cat#: S11222
HCR probe		
Mm-Trpm8 v3.0	Molecular Instruments	
Chemicals		
Cholera toxin B subunit	Sigma-Aldrich	Cat#: C9972
DAPI	Sigma-Aldrich	Cat#: D9542
Sodium borohydride	Sigma-Aldrich	Cat#: 452882
3,3'-Diaminobenzidine	Revvity	Cat#: NEL938001EA
Hydrogen peroxide	Sigma-Aldrich	Cat#: H1009
Osmium tetroxide	Agar Scientific	Cat#: R1016
Uranyl acetate	Agar Scientific	Cat#: R1260A
Lead citrate	Agar Scientific	Cat#: R1210
Software		
Neurolucida	MBF Bioscience	https://www.mbfbioscience.com/neurolucida RRID: SCR_001775
Neurolucida Explorer	MBF Bioscience	https://www.mbfbioscience.com/neurolucida-explorer RRID: SCR_017348
pClamp	Molecular Devices	https://www.moleculardevices.com/products/axon-patch-clamp-system/acquisition-and-analysis-software/pclamp-software-suite#gref RRID: SCR_011323
Easy Electrophysiology	Easy Electrophysiology LTD	https://www.easyelectrophysiology.com
Zen Black	Carl Zeiss	https://www.zeiss.com/microscopy/int/products/microscope-software/zen.html RRID: SCR_018163
Prism	GraphPad Software	https://www.graphpad.com/scientific-software/prism/ RRID: SCR_002798
Photoshop CS6	Adobe Systems Incorporated	https://www.adobe.com/
Xara Xtreme v2.0	Xara Group Ltd	https://www.xara.com/
Inkscape	Software Freedom Conservancy	https://inkscape.org/

588 **Experimental Model and Subject Details**

589 All experiments were approved by the Ethical Review Process Applications Panel of the
590 University of Glasgow, and were carried out in accordance with the UK Animals (Scientific
591 Procedures) Act 1986 and ARRIVE guidelines. The following transgenic mouse lines were
592 used in this study: the BAC transgenic Phox2a::Cre line, which expresses Cre
593 recombinase under control of the Phox2a promoter[14]; the Ai9 Cre reporter line, in which a
594 loxP-flanked STOP cassette prevents CAG promoter-driven transcription of tdTomato[69];
595 the Trpm8^{Flp} line, in which 2A-linked FlpO recombinase is fused with the last codon (and
596 replaces the stop codon) of the *Trpm8* gene[13]; the RCE:FRT line, which carries the R26R
597 CAG-boosted EGFP reporter allele with a FRT-flanked STOP cassette upstream of the
598 EGFP gene[74]; and the Calb1^{Cre} line which has an IRES2 sequence and a Cre
599 recombinase gene inserted downstream of the translational STOP codon of the calbindin 1
600 gene[75]. Further details of these lines can be found in the Key Resources table. The
601 following crosses were generated by cross-breeding these lines: Trpm8^{Flp};RCE:FRT mice,
602 which were used for anatomical analysis of Trpm8-expressing DRG cells, for
603 electrophysiological experiments, and for retrograde tracing of spinothalamic neurons;
604 Trpm8^{Flp};RCE:FRT;Ai9 mice, which were used for some electrophysiological experiments;
605 Trpm8^{Flp};RCE:FRT;Phox2a::Cre;Ai9 mice, which were used for the combined confocal and
606 electron microscopic analysis; and Calb1^{Cre};Trpm8^{Flp};RCE:FRT mice, which were used to
607 determine the proportion of retrogradely labelled Calb1-expressing cells that received
608 dense Trpm8 input.

609 Perfusion fixation was performed while mice were deeply anaesthetised with
610 pentobarbitone (20 mg i.p.). A brief rinse with Ringer's solution was followed by perfusion
611 with ~250 ml of fixative. In all cases apart from those used for combined confocal/electron
612 microscopy the fixative consisted of 4% freshly depolymerised formaldehyde in phosphate
613 buffer (PB). Spinal cords and brains were dissected and stored in the same fixative for 2
614 hours, before being transferred to 30% sucrose in PB.

615 Dorsal root ganglia for FISH were obtained from Trpm8^{Flp};RCE:FRT mice, which had
616 been killed with an overdose of pentobarbital (40 mg i.p.) and perfused with cold
617 phosphate buffered saline (PBS). The ganglia were fixed in 4% formaldehyde for 2 hours.

618 Mice of both sexes, aged 4-14 weeks and weighing between 13 and 25 g at the start of
619 any surgical procedures were used in the study.

620

621 **Fluorescent *in situ* hybridisation, immunohistochemistry and imaging**

622 FISH was performed on intact lumbar dorsal root ganglia from Trpm8^{Flp};RCE:FRT mice
623 using HCR RNA-FISH v3.0 reagents. Tissues were dehydrated in graded ethanol
624 solutions, followed by rinsing in PBS. Hybridisation and amplification were performed with
625 a probe against mouse *Trpm8* mRNA and hairpins conjugated to Alexa Fluor 546 (HCR
626 v3.0, Molecular Instruments, Inc.) according to the manufacturer's instructions. Tissues
627 were mounted using antifade mounting medium and stored at -20°C.

628 Sections of brain, spinal cord and dorsal root ganglia for immunohistochemical
629 processing were cut on either a vibrating blade microtome (Leica VT1000 or VT1200) or a
630 cryostat (Leica CM1950). Section thickness was 50 µm for brain and 60 µm for spinal cord
631 and dorsal root ganglia. Multiple-label immunofluorescence microscopy was carried out as
632 described previously[5,59,76]. Reactions were performed on free-floating sections, and the
633 sources and concentrations of antibodies are listed in the Key Resources Table. Sections
634 were incubated for 1-3 days at 4°C or room temperature in primary antibodies diluted in
635 PBS that contained 0.3M NaCl, 0.3% Triton X-100 (except for tissue processed by the
636 confocal/EM method) and 5% normal donkey serum. After rinsing they were incubated for
637 2-18 hours in appropriate species-specific secondary antibodies that were raised in
638 donkey and conjugated to Alexa Fluor Plus 405, Alexa Fluor 488, Alexa Fluor Plus 488,
639 Alexa Fluor Plus 555, Alexa Fluor 647 or Rhodamine Red, in the same diluent. Following
640 the reaction, sections were mounted with anti-fade medium and stored at -20°C.

641 Tissue sections and dorsal root ganglia that had undergone immunofluorescence
642 labelling or FISH were scanned with either a Zeiss LSM710 confocal microscope with
643 Argon multi-line, 405 nm diode, 561 nm solid state and 633 nm HeNe lasers, or with a
644 Zeiss LSM900 Airyscan confocal microscope with 405, 488, 561 and 640 nm diode lasers.
645 Confocal image stacks were obtained through a 20x dry lens (numerical aperture, NA,
646 0.8), or through 40x (NA 1.3) or 63x (NA 1.4) oil immersion lenses with the confocal
647 aperture set to 1 Airy unit or less.

648 The method for combining confocal and electron microscopy was the same as that
649 described previously[77]. Two Trpm8^{Flp};RCE:FRT;Phox2a::Cre;Ai9 mice were perfused with
650 fixative that contained 0.5% glutaraldehyde and 4% formaldehyde. Horizontal sections of
651 spinal cord were obtained from lumbar segments, and these were treated with 50%
652 ethanol for 30 mins, to enhance antibody penetration, and then with 1% sodium
653 borohydride for 30 mins to quench unbound aldehyde sites. After rinsing, they were
654 incubated for 3 days in primary antibodies against GFP (raised in rabbit) and mCherry

Click here to enter text.

655 (raised in rat), and then overnight in a mixture of secondary antibodies: donkey anti-rabbit
656 conjugated to Alexa Fluor 488, donkey anti-rabbit conjugated to biotin and donkey anti-rat
657 conjugated to Rhodamine Red. Note that the anti-mCherry antibody recognises tdTomato.
658 The antibody diluent consisted of PBS that contained 0.3M NaCl and 5% normal donkey
659 serum. They were then incubated in avidin conjugated to horseradish peroxidase (HRP)
660 and mounted on slides with anti-fade medium. Sections were viewed with a confocal
661 microscope, and regions that contained tdTomato-positive cells that were densely coated
662 with GFP-labelled axons were selected. These were scanned with the confocal
663 microscope to generate z-series through the cell bodies and dendritic trees of the neurons.
664 The sections were then removed from the slides, rinsed in PBS and then PB, processed
665 with 3,3'-diaminobenzidine (DAB) and H_2O_2 to reveal peroxidase-labelled (Trpm8-positive)
666 axons, osmicated, stained with uranyl acetate, dehydrated and flat-embedded in Durcupan
667 resin between acetate sheets[77]. Series of ultrathin sections (silver interference colour)
668 were cut with a diamond knife and collected on Formvar-coated slot grids. These were
669 further stained with lead citrate and viewed with either a Philips CM100 or Jeol JEM-
670 1400Flash electron microscope.
671
672 **Intracranial and intraspinal injections**
673 All surgical procedures involving intraspinal and/or intracranial injections were
674 performed while the mice were anaesthetised with isoflurane (1-2%), and all animals
675 received perioperative analgesia (buprenorphine 0.1 mg/kg and carprofen 10 mg/kg, s.c.).
676 For both types of injection, the mice were placed in a stereotaxic frame.
677 For intracranial injections, lidocaine (10 mg/kg, s.c.) was injected into the skin over the
678 skull, which was then incised. Burr holes were drilled to allow targeting at the following co-
679 ordinates (CVLM: 1.1-1.3 mm lateral to midline, 3.5 mm caudal to lambdoid suture, 3.3-3.7
680 mm below brain surface; LPB: 1.1 mm lateral to the midline, 0.35 mm caudal to lambdoid
681 suture or 4.5 mm caudal to bregma, 3.0 mm below brain surface, PAG: 0.4 mm lateral to
682 midline, 0.4 mm caudal to the interaural line, 3.1 mm below brain surface; VPL: 1.6-1.7
683 lateral to the midline, 0.79-1.11 caudal to bregma, 3.4 mm below brain surface). Injections
684 were made through glass micropipettes (outer tip diameter ~60 μm) attached to a Harvard
685 Pump 11 Elite (for AAV injections) or a PV 800 Pneumatic Picopump (WPI; for CTB
686 injections). For optogenetic experiments, Trpm8^{Flp}RCE:FRT mice that had received
687 intraperitoneal injections of AAV.PHP.S.Flp^{ON}.ChR2_YFP (see below) were injected with
688 AAV11.tdTomato (2.5×10^9 GC in 500 nl) into the LPB or CVLM. Brain injections for the

689 electrophysiological experiments in which the semi-intact preparation was used to record
690 from cells with or without dense Trpm8 input consisted of AAV9.mCherry (7.5×10^{8}-
691 1.2×10^{10} GC in 500 nl) injected into the LPB or CVLM of Trpm8^{Flp};RCE:FRT mice, or
692 AAV9.Cre_GFP (3.5×10^{9} GC in 500 nl) injected into the CVLM of a Trpm8^{Flp};RCE:FRT;Ai9
693 mouse. For anatomical experiments involving Calb1^{Cre};Trpm8^{Flp};RCE:FRT mice
694 AAV11.Cre^{ON}.tdTomato was injected into LPB (2×10^{9} GC in 400 nl) or PAG (1×10^{9} GC in
695 200 nl). For the immunohistochemical analysis of calbindin expression in Trpm8-
696 innervated neurons, Trpm8^{Flp};RCE:FRT mice received injections of AAV9.mCherry
697 (7.5×10^{8}-1.2×10^{10} GC in 500 nl) into the LPB. For electrophysiological recording of Calb1-
698 expressing neurons in the semi-intact preparation, 4 Calb1^{Cre} mice were injected with
699 AAV11.Cre^{ON}.tdTomato into the CVLM (2×10^{9} GC in 400 nl). Injections into the lateral
700 thalamus consisted of 100 nl of 1% CTB. Micropipettes were left in place for ~5 mins after
701 the injection to limit leakage up the track. For electrophysiological experiments mice were
702 allowed to recover for between 9 and 22 days (see below for further details). For
703 anatomical experiments, survival times were 3 days for CTB injections and 12-16 days for
704 AAV injections and these were followed by perfusion fixation, as described above.
705 For intraspinal injections in lumbar spinal cord the T12 and L1 vertebrae were exposed
706 and clamped. Injections were made through glass micropipettes (outer tip diameter ~60
707 μm) attached to a 10 μL Hamilton syringe, on the right side of the spinal cord into either
708 the L3 segment, or the L3, L4 and L5 segments. Injections into L3 and L5 were made
709 through the intervertebral spaces on either side of the T13 vertebra, while those into L4
710 were made through a small hole drilled in the lamina of the T13 vertebra. In initial
711 experiments we used a similar strategy to that described in previous papers[5,64], and these
712 are referred to as “central” injections. We subsequently modified the technique in order to
713 restrict injection sites to the medial part of the dorsal horn and exclude the LSN, and we
714 refer to these as “medial” injections. For cervical injections, the head was held in place
715 with ear-bars and the T2 spine was clamped. Injections were made (as described above)
716 in the intervertebral space between the C6 and C7 vertebrae. The mice survived between
717 26 and 57 days and were then deeply anaesthetised and perfused with fixative as
718 described above (for further details see Table 1).
719
720 **Image analysis**
721 Lamina I ALS neurons that received numerous contacts from GFP-positive (Trpm8-
722 expressing) primary afferents were identified in several parts of this study, either following

Click here to enter text.

723 retrograde labelling or through expression of tdTomato (in crosses that involved
724 Phox2a::Cre and Ai9). The cells could be readily identified by the close association of
725 GFP-labelled axons with their dendrites, which received multiple contacts from GFP-
726 positive boutons. In most cases the cell bodies were also associated with numerous GFP-
727 labelled boutons, and these sometimes completely surrounded the cell body[13].
728 All quantitative image analyses were performed with Neurolucida for Confocal software
729 (MBF Bioscience, Williston, VT, USA).
730 To determine the proportion of DRG neurons that were labelled with GFP in
731 Trpm8^{Flp};RCE:FRT mice we scanned 3 or 4 sections immunostained to reveal GFP and
732 NeuN, and counterstained with DAPI from the L4 dorsal root ganglia from each of 3 mice
733 (1 male, 2 female) with a confocal microscope. Z-stacks that included the complete cross-
734 sectional area of the ganglion were analysed using a modified disector method[78].
735 Reference and look-up sections were set 10 µm apart, and all intervening sections were
736 examined to reveal any neurons that might have been located between these two levels.
737 Initially we viewed the NeuN and DAPI channels, and in this way, we identified all neurons
738 (between 904 and 1383 per mouse) for which the top surface of the nucleus was located
739 between reference and look-up section. We then revealed the channel for GFP and
740 counted any of the sampled neurons that were GFP-immunoreactive.
741 For the comparison of *Trpm8* mRNA and GFP dorsal root ganglia from 3
742 Trpm8^{Flp};RCE:FRT mice (1 male, 2 female) that had been reacted as described above
743 were scanned with a confocal microscope to generate z-series through the entire volume
744 of the ganglion. Initially, both fluorescent channels (GFP and Alexa Fluor 546) were
745 combined such that any cell with either GFP or *Trpm8* mRNA was visible. For all of these
746 cells (between 155-209 per mouse), the cell size was determined by drawing an outline of
747 the cell at its maximum point and converting cross-sectional area to diameter by assuming
748 a circular shape. The two fluorescent channels were then separated, and for each cell the
749 presence of GFP and/or *Trpm8* mRNA was determined.
750 Because we found a relatively limited range of sizes for GFP/*Trpm8*-positive cells (see
751 Figure 1C) we did not use a stereological method for analysing co-localisation with other
752 neurochemical markers. We scanned sections of dorsal root ganglia immunoreacted to
753 reveal GFP together with: (1) VGLUT3, (2) Trpv1, (3) CGRP and substance P, or (4)
754 somatostatin. In each case tissue from 3 mice (either 2 male and 1 female, or 1 male and
755 2 female) was used, and z-stacks covering the entire cross-sectional area of the ganglion
756 were analysed. Initially the GFP channel was viewed and the locations of all labelled cells

Click here to enter text.

757 were marked (between 126 and 350 per mouse for each reaction). The other channel(s)
758 was/were then examined and the presence or absence of the other marker(s) was noted.
759 To determine the proportion of retrogradely labelled lamina I neurons that had dense
760 input from Trpm8-expressing afferents in the Calb1^{Cre};Trpm8^{Flp};RCE:FRT mice injected
761 with AAV11.Cre^{ON}.tdTomato into either LPB (4 mice, 2 male and 2 female) or PAG (3
762 mice, 1 male, 2 female), we examined horizontal sections cut through the L2, L3 and L4
763 segments. These had been immunostained to reveal GFP and tdTomato, and were
764 scanned with a confocal microscope. The resulting z-stacks were viewed with Neurolucida
765 software, initially with only the tdTomato channel visible, and the locations of retrogradely
766 labelled lamina I neurons were recorded (between 32 and 81 cells per segment in each
767 animal for the experiments involving LPB injections). For the experiments involving PAG
768 injections, numbers of retrogradely labelled neurons were much lower, and results from
769 the 3 segments were pooled for each animal (between 26 and 99 cells per mouse). The
770 GFP channel was then viewed, and cells that received dense Trpm8 input were identified.
771 The L5 segments of the 4 Calb1^{Cre};Trpm8^{Flp};RCE:FRT mice that had received injections
772 into LPB mice were cut transversely and the locations of tdTomato-labelled cell bodies on
773 between 8 and 10 individual sections were identified. These were then morphed onto a
774 standard outline of the L5 segment in Inkscape, resulting in single scalable vector graphics
775 files for each mouse.
776 To test whether cold-selective cells were included among those projecting to the lateral
777 thalamus, we examined horizontal sections from the L4 and C7 segments of 3
778 Trpm8^{Flp};RCE:FRT mice (2 male, 1 female) that had received CTB injections into the
779 lateral thalamus. Sections were immunoreacted to reveal CTB and GFP and scanned with
780 a confocal microscope. We then searched for CTB-labelled cells that were associated with
781 numerous GFP-positive axons.
782 For anterograde tracing following intraspinal injections of AAV1.Cre^{ON}.tdTomato in
783 Calb1^{Cre} mice, sections were first viewed with a fluorescence microscope (Zeiss Axioscope
784 5) and selected sections were scanned with a confocal microscope. Identification of brain
785 regions that contained tdTomato-labelled axons was generally based on the atlas of
786 Franklin and Paxinos[62], apart from the LPB. For this, we used the same terminology as in
787 our previous paper[64], and identified the PBrel nucleus based on the findings of Geerling et
788 al[49].
789

790 **Whole spinal cord preparation**

791 The whole spinal cord preparation was made as described previously with minor
792 modifications[44]. Animals were anaesthetised with isoflurane, followed by a lethal dose of
793 pentobarbital, and then quickly perfused with oxygenated sucrose-based artificial
794 cerebrospinal fluid (ACSF; in mM; 3.0 KCl, 1.2 NaH2PO4, 0.5 CaCl2, 7.0 MgCl2, 26.0
795 NaHCO3, 15.0 glucose, 251.6 sucrose, 1.0 Na ascorbate, and 1.0 Na pyruvate).
796 Immediately after perfusion, the back skin was incised and the spinal cord was quickly
797 excised and placed into a sucrose-based ACSF. Dura and pia-arachnoid membranes were
798 removed. The spinal cord was pinned into a chamber wall made from Sylgard.The spinal
799 cord was perfused with oxygenated normal ACSF (in mM; 125.8 NaCl, 3.0 KCl, 1.2
800 NaH_2PO_4, 2.4 $CaCl_2$, 1.3 $MgCl_2$, 26.0 $NaHCO_3$, and 15.0 glucose) at 25˚C.
801

802 **Semi-intact somatosensory preparation**

803 The semi-intact somatosensory preparation was made as described previously[31,32] with
804 minor modifications. Mice were anaesthetised with isoflurane, followed by a lethal dose of
805 pentobarbital, and then quickly perfused with oxygenated sucrose-based artificial
806 cerebrospinal fluid (ACSF; in mM; 3.0 KCl, 1.2 NaH_2PO_4, 0.5 $CaCl_2$, 7.0 $MgCl_2$, 26.0
807 $NaHCO_3$, 15.0 glucose, 251.6 sucrose, 1.0 Na ascorbate, and 1.0 Na pyruvate). The back
808 skin was incised, and the spinal cord was exposed by dorsal laminectomy. The right
809 hindlimb and the right side of the trunk with the spinal cord were excised and transferred to
810 the dissection/recording chamber, and tissues were submerged in the oxygenated
811 sucrose-based ACSF. The right hind paw skin, saphenous nerve, and femoral cutaneous
812 nerve were carefully isolated from the surrounding tissues. Only the L2 and L3 ganglia on
813 the right side were left attached to the spine. All dorsal roots except L2 and L3, dural and
814 pial membranes were carefully removed. The spinal cord was pinned onto a Sylgard
815 chamber with the right dorsal horn facing upward. The tissued was perfused with
816 oxygenated normal ACSF (in mM; 125.8 NaCl, 3.0 KCl, 1.2 NaH_2PO_4, 2.4 $CaCl_2$, 1.3
817 $MgCl_2$, 26.0 $NaHCO_3$, and 15.0 glucose) at 25˚C. Recordings were performed for up to 4
818 hours after dissection. The hindpaw skin was also at a temperature of 25˚C. At this
819 temperature Trpm8 afferents will have been active, but are likely to have adapted over the
820 course of the experiment. In addition, the conduction velocity of their axons will have been
821 lower than in the *in vivo* state.
822

823 **Patch-clamp recording from lamina I projection neurons**

824 Neurons were visualised using a fixed stage upright microscope (SliceScope;
825 Scientifica, Uckfield, UK) equipped with a 40x water immersion objective and a CMOS
826 Camera (Prime BSI Express, Teledyne Vision Solutions, Ontario, Canada). A narrow-
827 beam infrared LED (Opto SFH 4550; Osram, Munich, Germany, emission peak, 860 nm)
828 was positioned outside the solution meniscus. Fluorescent cells and axons were visualised
829 using LED illumination (pE-300 ultra, CoolLED, Andover, UK). Whole-cell patch clamp
830 recordings were made with a pipette constructed from thin-walled single-filamented
831 borosilicate glass using a microelectrode puller (P-1000, Sutter Instrument, CA, USA).
832 Pipette resistances ranged from 6 to 10 MΩ. Electrodes were filled with an intracellular
833 solution (in mM; 130.0 K gluconate, 10.0 KCl, 2.0 $MgCl_2$, 10.0 HEPES, 0.5 EGTA, 2.0
834 ATP-Na, 0.5 GTP-Na, and 0.2% Neurobiotin, pH adjusted to 7.3 with 1.0 M KOH). Data
835 were recorded and acquired with an amplifier (Axopatch 200B; Molecular Devices,
836 Wokingham, UK). The data were low-pass filtered at 2 kHz and digitised at 10 kHz with an
837 A/D converter (Digidata 1550B; Molecular Devices, Wokingham, UK) and stored using a
838 data acquisition program (Clampex 11; Molecular Devices, Wokingham, UK).
839

840 **Optogenetic activation**

841 Two $Trpm8^{Flp}$;RCE:FRT mice were given intraperitoneal injections of
842 AAV.PHP.S.Flp^{ON}.ChR2_YFP (1.3×10^{11} GC in 10 µl) on postnatal day 2 and 5 weeks later
843 they received brain injections of AAV11.tdTomato, as described above. A blue light pulse
844 (pE-300 ultra, CoolLED, Andover, UK) was applied through the objective (40x) of the
845 microscope for 1 ms. The shutter was controlled by a TTL pulse from the A/D converter
846 (Digidata 1550B; Molecular Devices, Wokingham, UK). To determine whether the
847 recorded neuron received monosynaptic or polysynaptic input from Trpm8 afferents, we
848 applied 0.2 Hz photostimulation (1 ms pulse width) based on a previous study[44] with minor
849 modifications. Input was considered monosynaptic if there was no failure and the latency
850 jitter was smaller than 1ms.
851

852 **Natural stimulation to the skin**

853 To test whether cells with dense Trpm8 input were cold-selective, we made patch-clamp
854 recordings in mice in which Trpm8 axons were revealed with GFP and projection neurons
855 were labelled with either mCherry or tdTomato using semi-intact somatosensory
856 preparation (Fig 4A). Successful recordings were made in 6 out of 16 experiments: 5

Click here to enter text.

857 Trpm8^{Flp};RCE:FRT mice (2 male, 3 female) that had received injections of AAV9.mCherry
858 into the LPB or CVLM, and one male Trpm8^{Flp};RCE:FRT;Ai9 mouse injected in the CVLM
859 with AAV9.EGFP_Cre. To test whether cells with dense Trpm8 input were cold-selective,
860 we made patch-clamp recordings in For the investigation of Calb1-Cre-positive lamina I
861 neurons, recordings were made in 4 female Calb1^{Cre} mice that had received injections of
862 AAV11.Cre^{ON}.tdTomato into the CVLM.
863 Recordings were initially made in voltage clamp mode (VH = -70mV) to reveal
864 spontaneous EPSCs. To find the receptive field of the recorded neurons, mechanical, hot,
865 and cold stimuli were gently applied to the skin. Mechanical stimulation was applied using
866 von Frey filaments (4-g or 10-g), and in some cases the skin was brushed with a
867 paintbrush. Hot and cold stimulation were administered by applying a small amount of
868 15˚C saline or 50˚C saline to the skin using an eye dropper. The temperature at the skin
869 surface was 20˚C and 38˚C, respectively. Once the receptive field was identified, each
870 stimulus was reapplied directly to the receptive field for 1 second. The evoked EPSCs
871 were recorded in voltage clamp mode (VH = -70mV), and the evoked action potentials
872 were recorded in current clamp mode (IH = 0 pA) or both. The events were detected with
873 Easy Electrophysiology software (Easy Electrophysiology, London, UK).
874
875 **Quantification and statistical analysis**
876 Data are reported as mean ± SD, unless stated otherwise. Statistical analyses were
877 performed using Prism software (v10, GraphPad Software, CA, USA) or SciPy library
878 (https://docs.scipy.org/doc/) in Python. The statistical tests used for each experiment,
879 including tests for multiple comparisons, are given in the appropriate figure legends. A p
880 value of <0.05 was considered significant, and significance markers are denoted within
881 figures as follows: *p < 0.05, **p < 0.01, ***p < 0.001.
882
883 **Data and materials availability**
884 Upon acceptance of this manuscript, all data will be made accessible from the Enlighten:
885 Research Data open repository hosted at the University of Glasgow. This study did not
886 generate any new materials, reagents or code.
887

ACKNOWLEDGMENTS

This research was funded in whole, or in part, by the Wellcome Trust (Grant numbers 219433/Z/19/Z and 304005/Z/23/Z) and the Medical Research Council (Grant number MR/V033638/1). For the purpose of Open Access, the authors have applied a CC BY public copyright licence to any Author Accepted Manuscript version arising from this submission. We are grateful to Robert Kerr, Iain Plenderleith and Erin Dunn for expert technical assistance, and to Mark Hoon and Artur Kania for the gifts of Trpm8^{Flp} and Phox2a::Cre mice.

AUTHOR CONTRIBUTIONS

A.N.R., W.M., A.C.D., E.P, A.M.B., A.J.T and J.H. conceived the project and designed experiments. A.J.T., A.M.B. and J.H. obtained funding. A.N.R., W.M., A.C.D., E.P., A.M., M.Y., A.H.C., D.S., A.M.B. and J.H. performed experiments. A.N.R., W.M., A.M., A.J.T. and J.H. analysed data. M.W. provided reagents. A.N.R., W.M., A.M.B., A.J.T. and J.H. wrote the paper. All of the authors provided feedback and contributed to editing of the manuscript.

COMPETING INTERESTS

The authors declare no competing interests.

Click here to enter text.

909 **REFERENCES**

910 1. Javed, S., Viswanathan, A., and Abdi, S. (2020). Cordotomy for intractable cancer pain: a narrative
911 review. Pain Physician *23*, 283-292.
912 2. Lahuerta, J., Bowsher, D., Campbell, J., and Lipton, S. (1990). Clinical and instrumental evaluation of
913 sensory function before and after percutaneous anterolateral cordotomy at cervical level in man.
914 Pain *42*, 23-30. 10.1016/0304-3959(90)91087-Y.
915 3. Chen, H., Bleimeister, I.H., Nguyen, E.K., Li, J., Cui, A.Y., Stratton, H.J., Smith, K.M., Baccei, M.L., and
916 Ross, S.E. (2024). The functional and anatomical characterization of three spinal output pathways of
917 the anterolateral tract. Cell reports *43*, 113829. 10.1016/j.celrep.2024.113829.
918 4. Ma, W., Dickie, A.C., Polgar, E., Yadav, M., Quillet, R., Gutierrez-Mecinas, M., Bell, A.M., and Todd,
919 A.J. (2025). Expression of Tacr1 and Gpr83 by spinal projection neurons. Molecular pain *21*,
920 17448069251342409. 10.1177/17448069251342409.
921 5. Ma, W., Polgar, E., Dickie, A.C., Hajer, M.A., Quillet, R., Gutierrez-Mecinas, M., Yadav, M.,
922 Hachisuka, J., Todd, A.J., and Bell, A.M. (2025). Anatomical characterisation of somatostatin-
923 expressing neurons belonging to the anterolateral system. Scientific reports *15*, 9549.
924 10.1038/s41598-025-93816-6.
925 6. McMahon, S.B., and Wall, P.D. (1983). A system of rat spinal cord lamina 1 cells projecting through
926 the contralateral dorsolateral funiculus. The Journal of comparative neurology *214*, 217-223.
927 10.1002/cne.902140209.
928 7. Chung, K., Kevetter, G.A., Willis, W.D., and Coggeshall, R.E. (1984). An estimate of the ratio of
929 propriospinal to long tract neurons in the sacral spinal cord of the rat. Neuroscience letters *44*, 173-
930 177. 10.1016/0304-3940(84)90077-6.
931 8. Abraira, V.E., and Ginty, D.D. (2013). The sensory neurons of touch. Neuron *79*, 618-639.
932 10.1016/j.neuron.2013.07.051.
933 9. Ma, Q. (2022). A functional subdivision within the somatosensory system and its implications for
934 pain research. Neuron *110*, 749-769. 10.1016/j.neuron.2021.12.015.
935 10. Todd, A.J. (2010). Neuronal circuitry for pain processing in the dorsal horn. Nature reviews.
936 Neuroscience *11*, 823-836. nrn2947 [pii] 10.1038/nrn2947.
937 11. Wang, L.H., Ding, W.Q., and Sun, Y.G. (2022). Spinal ascending pathways for somatosensory
938 information processing. Trends Neurosci *45*, 594-607. 10.1016/j.tins.2022.05.005.
939 12. Wercberger, R., and Basbaum, A.I. (2019). Spinal cord projection neurons: a superficial, and also
940 deep, analysis. Curr Opin Physiol *11*, 109-115. 10.1016/j.cophys.2019.10.002.
941 13. Bell, A.M., Utting, C., Dickie, A.C., Kucharczyk, M.W., Quillet, R., Gutierrez-Mecinas, M., Razlan,
942 A.N.B., Cooper, A.H., Lan, Y., Hachisuka, J., et al. (2024). Deep sequencing of Phox2a nuclei reveals
943 five classes of anterolateral system neurons. Proceedings of the National Academy of Sciences of
944 the United States of America *121*, e2314213121. 10.1073/pnas.2314213121.
945 14. Roome, R.B., Bourojeni, F.B., Mona, B., Rastegar-Pouyani, S., Blain, R., Dumouchel, A., Salesse, C.,
946 Thompson, W.S., Brookbank, M., Gitton, Y., et al. (2020). Phox2a defines a developmental origin of
947 the anterolateral system in mice and humans. Cell reports *33*, 108425.
948 10.1016/j.celrep.2020.108425.
949 15. Peier, A.M., Moqrich, A., Hergarden, A.C., Reeve, A.J., Andersson, D.A., Story, G.M., Earley, T.J.,
950 Dragoni, I., McIntyre, P., Bevan, S., and Patapoutian, A. (2002). A TRP channel that senses cold
951 stimuli and menthol. Cell *108*, 705-715. 10.1016/s0092-8674(02)00652-9.
952 16. McKemy, D.D., Neuhausser, W.M., and Julius, D. (2002). Identification of a cold receptor reveals a
953 general role for TRP channels in thermosensation. Nature *416*, 52-58. 10.1038/nature719.
954 17. Lewis, C.M., and Griffith, T.N. (2022). The mechanisms of cold encoding. Current opinion in
955 neurobiology *75*, 102571. 10.1016/j.conb.2022.102571.
956 18. Knowlton, W.M., Palkar, R., Lippoldt, E.K., McCoy, D.D., Baluch, F., Chen, J., and McKemy, D.D.
957 (2013). A sensory-labeled line for cold: TRPM8-expressing sensory neurons define the cellular basis

958 for cold, cold pain, and cooling-mediated analgesia. The Journal of neuroscience : the official
959 journal of the Society for Neuroscience *33*, 2837-2848. 10.1523/JNEUROSCI.1943-12.2013.
960 19. Pogorzala, L.A., Mishra, S.K., and Hoon, M.A. (2013). The cellular code for mammalian
961 thermosensation. The Journal of neuroscience : the official journal of the Society for Neuroscience
962 *33*, 5533-5541. 10.1523/JNEUROSCI.5788-12.2013.
963 20. Takashima, Y., Daniels, R.L., Knowlton, W., Teng, J., Liman, E.R., and McKemy, D.D. (2007). Diversity
964 in the neural circuitry of cold sensing revealed by genetic axonal labeling of transient receptor
965 potential melastatin 8 neurons. The Journal of neuroscience : the official journal of the Society for
966 Neuroscience *27*, 14147-14157. 10.1523/JNEUROSCI.4578-07.2007.
967 21. Kim, Y.S., Park, J.H., Choi, S.J., Bae, J.Y., Ahn, D.K., McKemy, D.D., and Bae, Y.C. (2014). Central
968 connectivity of transient receptor potential melastatin 8-expressing axons in the brain stem and
969 spinal dorsal horn. PloS one *9*, e94080. 10.1371/journal.pone.0094080.
970 22. Dhaka, A., Earley, T.J., Watson, J., and Patapoutian, A. (2008). Visualizing cold spots: TRPM8-
971 expressing sensory neurons and their projections. The Journal of neuroscience : the official journal
972 of the Society for Neuroscience *28*, 566-575. 28/3/566 [pii] 10.1523/JNEUROSCI.3976-07.2008.
973 23. Craig, A.D., and Kniffki, K.D. (1985). Spinothalamic lumbosacral lamina I cells responsive to skin and
974 muscle stimulation in the cat. The Journal of physiology *365*, 197-221.
975 10.1113/jphysiol.1985.sp015767.
976 24. Craig, A.D., Krout, K., and Andrew, D. (2001). Quantitative response characteristics of
977 thermoreceptive and nociceptive lamina I spinothalamic neurons in the cat. Journal of
978 neurophysiology *86*, 1459-1480. 10.1152/jn.2001.86.3.1459.
979 25. Craig, A.D., and Dostrovsky, J.O. (2001). Differential projections of thermoreceptive and nociceptive
980 lamina I trigeminothalamic and spinothalamic neurons in the cat. Journal of neurophysiology *86*,
981 856-870. 10.1152/jn.2001.86.2.856.
982 26. Craig, A.D., and Hunsley, S.J. (1991). Morphine enhances the activity of thermoreceptive cold-
983 specific lamina I spinothalamic neurons in the cat. Brain research *558*, 93-97. 10.1016/0006-
984 8993(91)90719-c.
985 27. Dostrovsky, J.O., and Craig, A.D. (1996). Cooling-specific spinothalamic neurons in the monkey.
986 Journal of neurophysiology *76*, 3656-3665. 10.1152/jn.1996.76.6.3656.
987 28. Zhang, X., Davidson, S., and Giesler, G.J., Jr. (2006). Thermally identified subgroups of marginal zone
988 neurons project to distinct regions of the ventral posterior lateral nucleus in rats. The Journal of
989 neuroscience : the official journal of the Society for Neuroscience *26*, 5215-5223.
990 10.1523/JNEUROSCI.0701-06.2006.
991 29. Allard, J. (2019). Physiological properties of the lamina I spinoparabrachial neurons in the mouse.
992 The Journal of physiology *597*, 2097-2113. 10.1113/JP277447.
993 30. Andrew, D. (2009). Sensitization of lamina I spinoparabrachial neurons parallels heat hyperalgesia
994 in the chronic constriction injury model of neuropathic pain. The Journal of physiology *587*, 2005-
995 2017.
996 31. Hachisuka, J., Baumbauer, K.M., Omori, Y., Snyder, L.M., Koerber, H.R., and Ross, S.E. (2016). Semi-
997 intact ex vivo approach to investigate spinal somatosensory circuits. Elife *5*, e22866.
998 10.7554/eLife.22866.
999 32. Hachisuka, J., Koerber, H.R., and Ross, S.E. (2020). Selective-cold output through a distinct subset of
1000 lamina I spinoparabrachial neurons. Pain *161*, 185-194. 10.1097/j.pain.0000000000001710.
1001 33. Chisholm, K.I., Lo Re, L., Polgar, E., Gutierrez-Mecinas, M., Todd, A.J., and McMahon, S.B. (2021).
1002 The encoding of cutaneous stimuli by lamina I projection neurons. Pain *162*, 2405-2417.
1003 10.1097/j.pain.0000000000002226.
1004 34. Lee, H., Hor, C.C., Horwitz, L.R., Xiong, A., Su, X.Y., Soden, D.R., Yang, S., Cai, W., Zhang, W., Li, C., et
1005 al. (2025). A dedicated skin-to-brain circuit for cool sensation in mice. Nature communications *16*,
1006 6731. 10.1038/s41467-025-61562-y.
1007 35. Qi, L., Iskols, M., Shi, D., Reddy, P., Walker, C., Lezgiyeva, K., Voisin, T., Pawlak, M., Kuchroo, V.K.,
1008 Chiu, I.M., et al. (2024). A mouse DRG genetic toolkit reveals morphological and physiological

1009 diversity of somatosensory neuron subtypes. Cell *187*, 1508-1526 e1516.
1010 10.1016/j.cell.2024.02.006.
1011 36. Sharma, N., Flaherty, K., Lezgiyeva, K., Wagner, D.E., Klein, A.M., and Ginty, D.D. (2020). The
1012 emergence of transcriptional identity in somatosensory neurons. Nature *577*, 392-398.
1013 10.1038/s41586-019-1900-1.
1014 37. Zeisel, A., Hochgerner, H., Lonnerberg, P., Johnsson, A., Memic, F., van der Zwan, J., Haring, M.,
1015 Braun, E., Borm, L.E., La Manno, G., et al. (2018). Molecular Architecture of the Mouse Nervous
1016 System. Cell *174*, 999-1014 e1022. 10.1016/j.cell.2018.06.021.
1017 38. Li, J., Kritzer, E., Craig, P.E., and Baccei, M.L. (2015). Aberrant synaptic integration in adult lamina I
1018 projection neurons following neonatal tissue damage. The Journal of neuroscience : the official
1019 journal of the Society for Neuroscience *35*, 2438-2451. 10.1523/JNEUROSCI.3585-14.2015.
1020 39. Seal, R.P., Wang, X., Guan, Y., Raja, S.N., Woodbury, C.J., Basbaum, A.I., and Edwards, R.H. (2009).
1021 Injury-induced mechanical hypersensitivity requires C-low threshold mechanoreceptors. Nature
1022 *462*, 651-655.
1023 40. Dickie, A.C., Bell, A.M., Iwagaki, N., Polgar, E., Gutierrez-Mecinas, M., Kelly, R., Lyon, H., Turnbull, K.,
1024 West, S.J., Etlin, A., et al. (2019). Morphological and functional properties distinguish the substance
1025 P and gastrin-releasing peptide subsets of excitatory interneuron in the spinal cord dorsal horn.
1026 Pain *160*, 442-462. 10.1097/j.pain.0000000000001406.
1027 41. Ordas, P., Hernandez-Ortego, P., Vara, H., Fernandez-Pena, C., Reimundez, A., Morenilla-Palao, C.,
1028 Guadano-Ferraz, A., Gomis, A., Hoon, M., Viana, F., and Senaris, R. (2021). Expression of the cold
1029 thermoreceptor TRPM8 in rodent brain thermoregulatory circuits. The Journal of comparative
1030 neurology *529*, 234-256. 10.1002/cne.24694.
1031 42. Gutierrez-Mecinas, M., Kuehn, E.D., Abraira, V.E., Polgár, E., Watanabe, M., and Todd, A.J. (2016).
1032 Immunostaining for Homer reveals the majority of excitatory synapses in laminae I-III of the mouse
1033 spinal dorsal horn. Neuroscience *329*, 171-181. 10.1016/j.neuroscience.2016.05.009.
1034 43. Todd, A.J. (1997). A method for combining confocal and electron microscopic examination of
1035 sections processed for double- or triple-labelling immunocytochemistry. Journal of neuroscience
1036 methods *73*, 149-157. S0165-0270(97)02222-X [pii].
1037 44. Hachisuka, J., Omori, Y., Chiang, M.C., Gold, M.S., Koerber, H.R., and Ross, S.E. (2018). Wind-up in
1038 lamina I spinoparabrachial neurons: a role for reverberatory circuits. Pain *159*, 1484-1493.
1039 10.1097/j.pain.0000000000001229.
1040 45. Menetrey, D., De Pommery, J., Thomasset, M., and Baimbridge, K.G. (1992). Calbindin-D28K
1041 (CaBP28k)-like Immunoreactivity in Ascending Projections. The European journal of neuroscience *4*,
1042 70-76. 10.1111/j.1460-9568.1992.tb00110.x.
1043 46. Alsulaiman, W.A.A., Quillet, R., Bell, A.M., Dickie, A.C., Polgar, E., Boyle, K.A., Watanabe, M.,
1044 Roome, R.B., Kania, A., Todd, A.J., and Gutierrez-Mecinas, M. (2021). Characterisation of lamina I
1045 anterolateral system neurons that express Cre in a Phox2a-Cre mouse line. Scientific reports *11*,
1046 17912. 10.1038/s41598-021-97105-w.
1047 47. Han, Z., Luo, N., Ma, W., Liu, X., Cai, Y., Kou, J., Wang, J., Li, L., Peng, S., Xu, Z., et al. (2023). AAV11
1048 enables efficient retrograde targeting of projection neurons and enhances astrocyte-directed
1049 transduction. Nature communications *14*, 3792. 10.1038/s41467-023-39554-7.
1050 48. Cano, G., Passerin, A.M., Schiltz, J.C., Card, J.P., Morrison, S.F., and Sved, A.F. (2003). Anatomical
1051 substrates for the central control of sympathetic outflow to interscapular adipose tissue during cold
1052 exposure. The Journal of comparative neurology *460*, 303-326. 10.1002/cne.10643.
1053 49. Geerling, J.C., Kim, M., Mahoney, C.E., Abbott, S.B., Agostinelli, L.J., Garfield, A.S., Krashes, M.J.,
1054 Lowell, B.B., and Scammell, T.E. (2016). Genetic identity of thermosensory relay neurons in the
1055 lateral parabrachial nucleus. Am J Physiol Regul Integr Comp Physiol *310*, R41-54.
1056 10.1152/ajpregu.00094.2015.
1057 50. Yang, W.Z., Xie, H., Du, X., Zhou, Q., Xiao, Y., Zhao, Z., Jia, X., Xu, J., Zhang, W., Cai, S., et al. (2023). A
1058 parabrachial-hypothalamic parallel circuit governs cold defense in mice. Nature communications
1059 *14*, 4924. 10.1038/s41467-023-40504-6.

Click here to enter text.

51. Yoshida, K., Konishi, M., Nagashima, K., Saper, C.B., and Kanosue, K. (2005). Fos activation in hypothalamic neurons during cold or warm exposure: projections to periaqueductal gray matter. Neuroscience *133*, 1039-1046. 10.1016/j.neuroscience.2005.03.044.
52. Vestergaard, M., Carta, M., Guney, G., and Poulet, J.F.A. (2023). The cellular coding of temperature in the mammalian cortex. Nature *614*, 725-731. 10.1038/s41586-023-05705-5.
53. Leva, T.M., and Whitmire, C.J. (2023). Thermosensory thalamus: parallel processing across model organisms. Front Neurosci *17*, 1210949. 10.3389/fnins.2023.1210949.
54. Bernard, J.F., Dallel, R., Raboisson, P., Villanueva, L., and Le Bars, D. (1995). Organization of the efferent projections from the spinal cervical enlargement to the parabrachial area and periaqueductal gray: a PHA-L study in the rat. The Journal of comparative neurology *353*, 480-505. 10.1002/cne.903530403.
55. Feil, K., and Herbert, H. (1995). Topographic organization of spinal and trigeminal somatosensory pathways to the rat parabrachial and Kolliker-Fuse nuclei. The Journal of comparative neurology *353*, 506-528. 10.1002/cne.903530404.
56. Gauriau, C., and Bernard, J.F. (2004). A comparative reappraisal of projections from the superficial laminae of the dorsal horn in the rat: the forebrain. The Journal of comparative neurology *468*, 24-56. 10.1002/cne.10873.
57. Gutierrez-Mecinas, M., Polgar, E., Bell, A.M., Herau, M., and Todd, A.J. (2018). Substance P-expressing excitatory interneurons in the mouse superficial dorsal horn provide a propriospinal input to the lateral spinal nucleus. Brain structure & function *223*, 2377-2392. 10.1007/s00429-018-1629-x.
58. Gutierrez-Mecinas, M., Bell, A., Polgar, E., Watanabe, M., and Todd, A.J. (2019). Expression of neuropeptide FF defines a population of excitatory interneurons in the superficial dorsal horn of the mouse spinal cord that respond to noxious and pruritic stimuli. Neuroscience *416*, 281-293. 10.1016/j.neuroscience.2019.08.013.
59. Polgár, E., Dickie, A.C., Gutierrez-Mecinas, M., Bell, A.M., Boyle, K.A., Quillet, R., Ab Rashid, E., Clark, R.A., German, M.T., Watanabe, M., et al. (2023). Grpr expression defines a population of superficial dorsal horn vertical cells that have a role in both itch and pain. Pain *164*, 149-170. 10.1097/j.pain.0000000000002677.
60. Choi, S., Hachisuka, J., Brett, M.A., Magee, A.R., Omori, Y., Iqbal, N.U., Zhang, D., DeLisle, M.M., Wolfson, R.L., Bai, L., et al. (2020). Parallel ascending spinal pathways for affective touch and pain. Nature *587*, 258-263. 10.1038/s41586-020-2860-1.
61. Al-Khater, K.M., Kerr, R., and Todd, A.J. (2008). A quantitative study of spinothalamic neurons in laminae I, III, and IV in lumbar and cervical segments of the rat spinal cord. The Journal of comparative neurology *511*, 1-18.
62. Franklin, K.B.J., and Paxinos, G. (2007). The Mouse Brain in Stereotaxic Coordinates. Third Edition (Elsevier).
63. Al-Khater, K.M., and Todd, A.J. (2009). Collateral projections of neurons in laminae I, III, and IV of rat spinal cord to thalamus, periaqueductal gray matter, and lateral parabrachial area. The Journal of comparative neurology *515*, 629-646.
64. Ma, W., Dickie, A., Polgar, E., Yadav, M., Quillet, R., Gutierrez-Mecinas, M., Bell, A.M., and Todd, A. (2025). Expression of Tacr1 and Gpr83 by spinal projection neurons. Molecular pain, 17448069251342409. 10.1177/17448069251342409.
65. Ding, Y.Q., Takada, M., Shigemoto, R., and Mizumo, N. (1995). Spinoparabrachial tract neurons showing substance P receptor-like immunoreactivity in the lumbar spinal cord of the rat. Brain research *674*, 336-340. 000689939500022I [pii].
66. Marshall, G.E., Shehab, S.A., Spike, R.C., and Todd, A.J. (1996). Neurokinin-1 receptors on lumbar spinothalamic neurons in the rat. Neuroscience *72*, 255-263. 0306452295005587 [pii].
67. McKemy, D.D. (2013). The molecular and cellular basis of cold sensation. ACS Chem Neurosci *4*, 238-247. 10.1021/cn300193h.

68. Ren, X., Liu, S., Virlogeux, A., Kang, S.J., Brusch, J., Liu, Y., Dymecki, S.M., Han, S., Goulding, M., and Acton, D. (2023). Identification of an essential spinoparabrachial pathway for mechanical itch. Neuron *111*, 1812-1829 e1816. 10.1016/j.neuron.2023.03.013.
69. Madisen, L., Zwingman, T.A., Sunkin, S.M., Oh, S.W., Zariwala, H.A., Gu, H., Ng, L.L., Palmiter, R.D., Hawrylycz, M.J., Jones, A.R., et al. (2010). A robust and high-throughput Cre reporting and characterization system for the whole mouse brain. Nature neuroscience *13*, 133-140. nn.2467 [pii] 10.1038/nn.2467.
70. Morrison, S.F. (2018). Efferent neural pathways for the control of brown adipose tissue thermogenesis and shivering. Handb Clin Neurol *156*, 281-303. 10.1016/B978-0-444-63912-7.00017-5.
71. Li, J., Serafin, E.K., and Baccei, M.L. (2023). Intrinsic and synaptic properties of adult mouse spinoperiaqueductal gray neurons and the influence of neonatal tissue damage. Pain *164*, 905-917. 10.1097/j.pain.0000000000002787.
72. Spike, R.C., Puskar, Z., Andrew, D., and Todd, A.J. (2003). A quantitative and morphological study of projection neurons in lamina I of the rat lumbar spinal cord. The European journal of neuroscience *18*, 2433-2448.
73. Chen, X.M., Nishi, M., Taniguchi, A., Nagashima, K., Shibata, M., and Kanosue, K. (2002). The caudal periaqueductal gray participates in the activation of brown adipose tissue in rats. Neuroscience letters *331*, 17-20. 10.1016/s0304-3940(02)00757-7.
74. Sousa, V.H., Miyoshi, G., Hjerling-Leffler, J., Karayannis, T., and Fishell, G. (2009). Characterization of Nkx6-2-derived neocortical interneuron lineages. Cerebral cortex *19 Suppl 1*, i1-10. 10.1093/cercor/bhp038.
75. Daigle, T.L., Madisen, L., Hage, T.A., Valley, M.T., Knoblich, U., Larsen, R.S., Takeno, M.M., Huang, L., Gu, H., Larsen, R., et al. (2018). A suite of transgenic driver and reporter mouse lines with enhanced brain-cell-type targeting and functionality. Cell *174*, 465-480 e422. 10.1016/j.cell.2018.06.035.
76. Quillet, R., Gutierrez-Mecinas, M., Polgar, E., Dickie, A.C., Boyle, K.A., Watanabe, M., and Todd, A.J. (2023). Synaptic circuits involving gastrin-releasing peptide receptor-expressing neurons in the dorsal horn of the mouse spinal cord. Front Mol Neurosci *16*, 1294994. 10.3389/fnmol.2023.1294994.
77. Bell, A.M., Gutierrez-Mecinas, M., Stevenson, A., Casas-Benito, A., Wildner, H., West, S.J., Watanabe, M., and Todd, A.J. (2020). Expression of green fluorescent protein defines a specific population of lamina II excitatory interneurons in the GRP::eGFP mouse. Scientific reports *10*, 13176. 10.1038/s41598-020-69711-7.
78. Polgár, E., Gray, S., Riddell, J.S., and Todd, A.J. (2004). Lack of evidence for significant neuronal loss in laminae I-III of the spinal dorsal horn of the rat in the chronic constriction injury model. Pain *111*, 144-150. 10.1016/j.pain.2004.06.011 S0304395904002994 [pii].

1148 **MAIN FIGURES**

1149 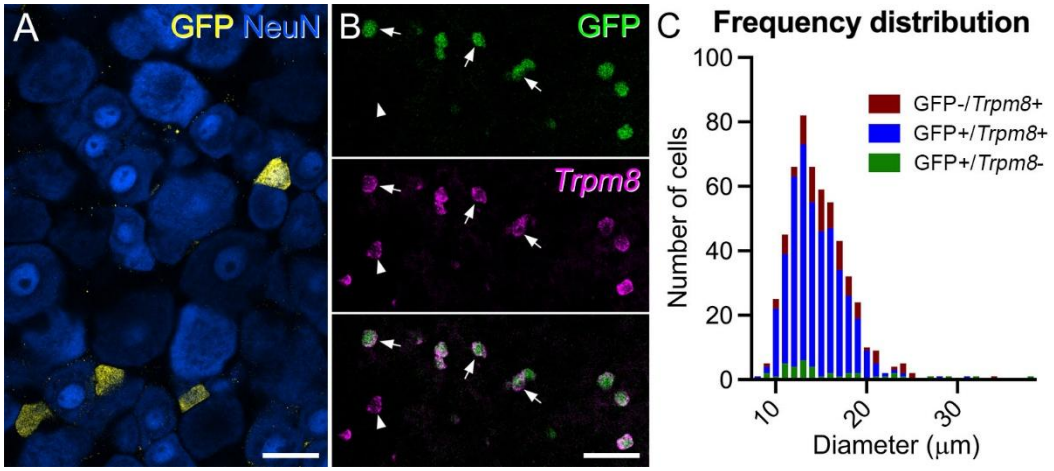

1150 **Figure 1. The Trpm8^{Flp} mouse line captures Trpm8-expressing primary afferent**
1151 **neurons.** (**A**) Immunohistochemical staining for GFP (yellow) and NeuN (blue) in a dorsal
1152 root ganglion from a Trpm8^{Flp};RCE:FRT mouse. GFP is present in some of the small
1153 neurons. (**B**) Fluorescence *in situ* hybridisation with a probe for *Trpm8* mRNA (magenta)
1154 superimposed on GFP native fluorescence (green). The great majority of GFP cells
1155 contain *Trpm8* message, and *vice versa*. Some of the double-labelled cells are indicated
1156 with arrows, while the arrowhead points to a *Trpm8*-positive cell that lacks GFP. (**C**)
1157 Frequency distribution of soma diameter for cells that were GFP-/*Trpm8*+ (red bars),
1158 GFP+/*Trpm8*+ (blue bars) or GFP+/*Trpm8*- (green bars). Scale bars: (**A**) = 25 μm, (**B**) = 50
1159 μm.

1160

Click here to enter text.

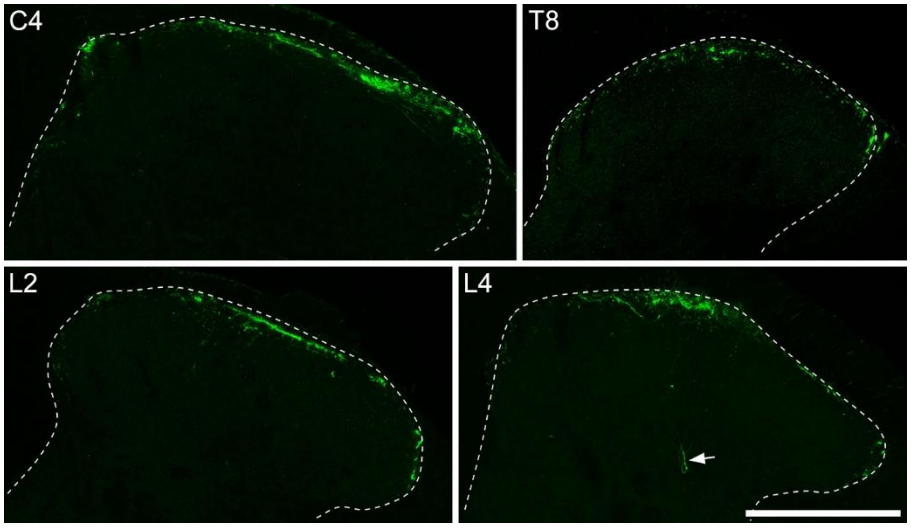

Figure 2. Distribution of Trpm8 afferents in the spinal dorsal horn.
Immunohistochemical staining for GFP at different segmental levels through the spinal cord in Trpm8^{Flp};RCE:FRT mice. GFP-labelled axons are largely restricted to lamina I, although occasional fibres penetrate into deeper parts of the dorsal horn (arrow). Within lamina I the distribution of GFP axons is patchy, and does not occupy the entire mediolateral extent. Scale bar = 200 μm.

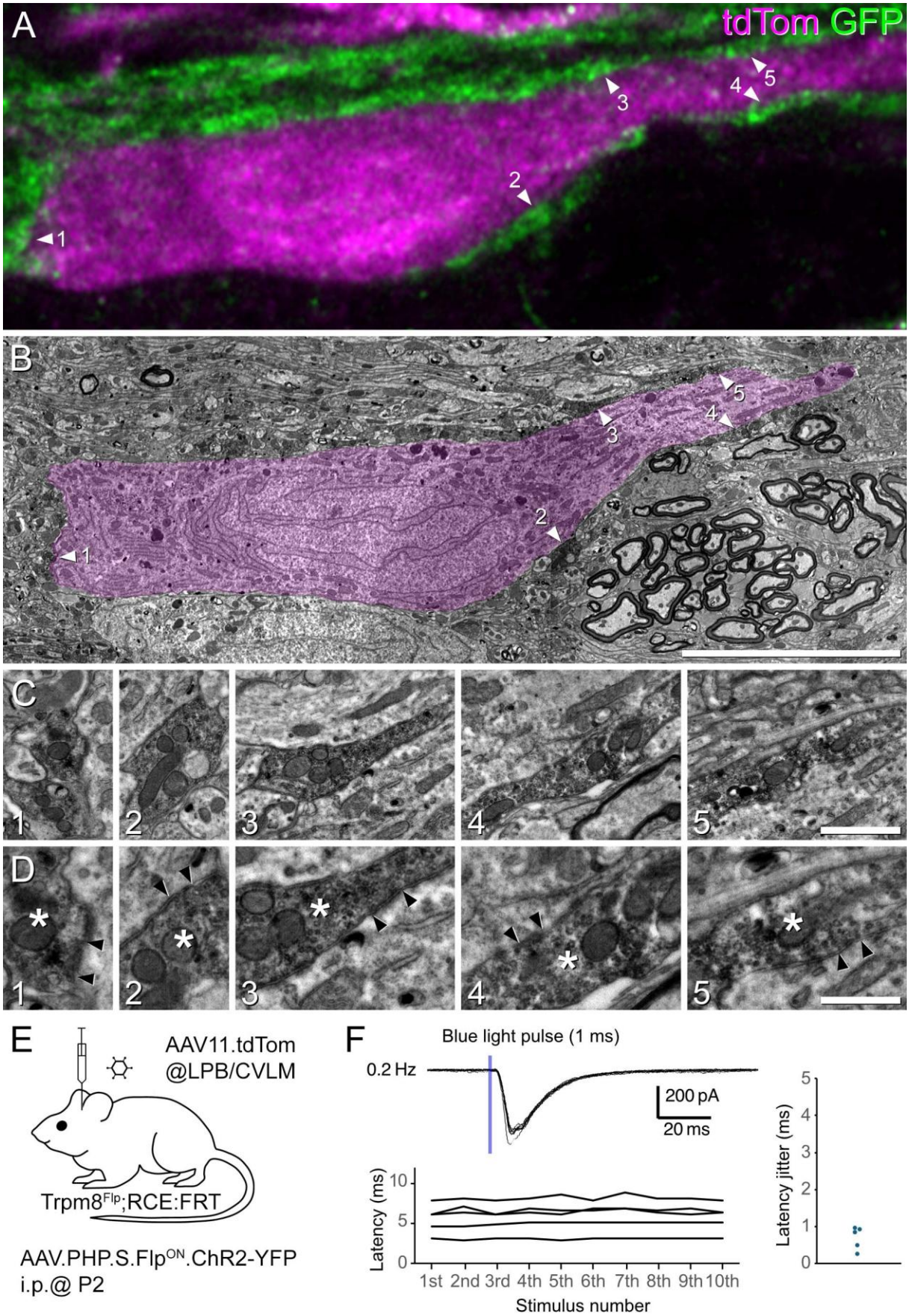

1170

Click here to enter text.

1171 **Figure 3. Evidence for monosynaptic input from Trpm8 afferents to lamina I ALS**
1172 **neurons that were surrounded by these afferents.** (**A**-**D**) Combined confocal and
1173 electron microscopic examination of a lamina I projection neuron with numerous contacts
1174 from Trpm8-expressing afferents. (**A**) A confocal image (single optical section) from a
1175 horizontal section through lamina I, showing the cell body and part of a proximal dendrite
1176 of one of the tdTomato-expressing neurons that were analysed. The tissue was obtained
1177 from a Phox2a::Cre;Ai9;Trpm8^{Flp};RCE:FRT mouse. TdTomato expressed by the projection
1178 neuron is shown in magenta and GFP immunoreactivity in Trpm8 afferents in green.
1179 Several Trpm8 boutons contact the cell, and five of these are indicated with arrowheads.
1180 (**B**) A low magnification electron micrograph through the cell at approximately the same z-
1181 level as that shown in **A**. Although the cell does not contain an electron dense label, it can
1182 be recognised by its shape, and because it is surrounded by GFP-expressing axonal
1183 profiles that were labelled with an immunoperoxidase method. The locations of those
1184 corresponding to the boutons shown in **A** are again marked with arrowheads. The cell has
1185 been pseudocoloured magenta to show its location. (**C**,**D**) Progressively higher
1186 magnification EM images showing the five GFP-labelled boutons marked with arrowheads
1187 in **A** and **B**. In **D** the boutons are marked with asterisks and the locations of membrane
1188 darkening and vesicle clusters that presumably correspond to synapses on the cell body
1189 and dendrite of the projection neuron are indicated with arrowheads. (**E**) The experimental
1190 approach used for optogenetic testing of Trpm8 input to ALS neurons. Stimulation (1 ms,
1191 0.2 Hz) evoked EPSCs in 5 of the ALS neurons that were densely coated by Trpm8
1192 afferents. (**F**) shows an example of the response in one cell (upper trace), the latencies of
1193 EPSCs in in response to 10 consecutive stimuli (n = 5, lower graph), and on the right, the
1194 latency jitter for each of these cells (n = 5). Scale bars: (**A**,**B**) = 10 μm, (**C**) = 1 μm (**D**) =
1195 500 nm.
1196

Click here to enter text.

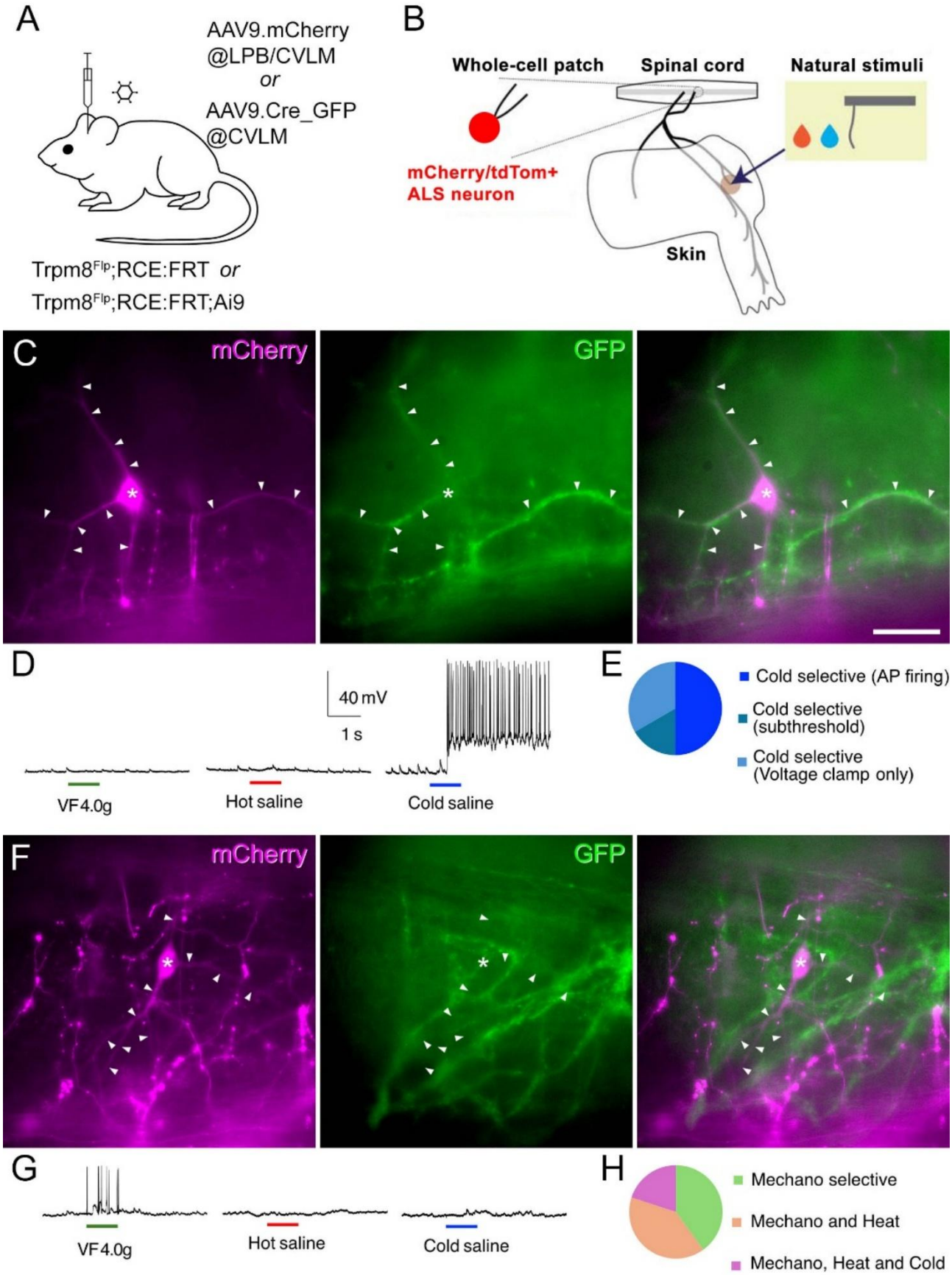

1197

1198 **Figure 4. Electrophysiological characterisation of retrogradely labelled lamina I**

1199 **projection neurons recorded in Trpm8^{Flp};RCE:FRT mice** (**A**) Cells were identified by

Click here to enter text.

1200 expression of mCherry following injection of AAV9.mCherry into the CVLM or LPB of
1201 Trpm8^{Flp};RCE:FRT mice, or by expression of tdTomato following injection of
1202 AAV9.Cre_GFP into the CVLM of Trpm8^{Flp};RCE:FRT;Ai9 mice. Note that the level of GFP
1203 expression resulting from injection of AAV9.Cre_GFP was extremely low, and would have
1204 been restricted to the nucleus of labelled neurons, due to the presence of a nuclear
1205 localisation signal. In both cases, Trpm8-expressing afferents were labelled with GFP. (**B**)
1206 The semi-intact somatosensory preparation retained skin attached to lumbar spinal cord
1207 through intact peripheral nerves and was used for recording responses to natural skin
1208 stimuli: Hot saline (50°C), Cold saline (15°C) or von Frey filaments (4 or 10 g) (**C**)
1209 Fluorescence microscopy image of a retrogradely labelled (mCherry-positive) lamina I ALS
1210 neuron (soma marked with asterisk) that is densely coated by Trpm8-expressing (GFP-
1211 positive) axons. Note that bundles of GFP axons are closely associated with the dendrites
1212 of the retrogradely labelled neuron, which are marked with arrowheads. (**D**) Whole-cell
1213 recording from this cell reveals that only cold stimulation evoked action potentials (APs).
1214 (**E**) Pie chart showing the response properties of the 6 lamina I ALS neurons that were
1215 densely coated with Trpm8 afferents to mechanical, cold and heat stimulation of the skin.
1216 All of these cells responded only to cold stimulation: 3 cells showed APs, 1 cell showed
1217 EPSPs but no APs (subthreshold), while 2 cells were recorded in voltage clamp and
1218 showed EPSCs. (**F**) Fluorescence microscopy image of a lamina I ALS neuron that was
1219 not densely coated with Trpm8 axons. Again, the soma is marked with an asterisk and
1220 dendrites with arrowheads. Note that although the dendrites of this cell pass through
1221 bundles of GFP axons these bundles are not aligned with the dendrites. (**G**) Whole-cell
1222 recording from the cell shown in (**F**). AP firing was evoked by mechanical stimulation (von
1223 Frey filament 4.0g), but not by application of hot or cold saline to the skin. (**H**) Pie chart of
1224 response properties of 5 lamina I ALS neurons that lacked dense Trpm8 input to
1225 mechanical, cold and heat stimulation to the skin. Two cells were mechano-selective, while
1226 three were polymodal (2 cells: mechano, heat, 1 cell: mechano, heat and cold). Scale bar
1227 (**C**,**F**) = 50 µm. Scale bars in **D** apply to **G**.
1228

1229

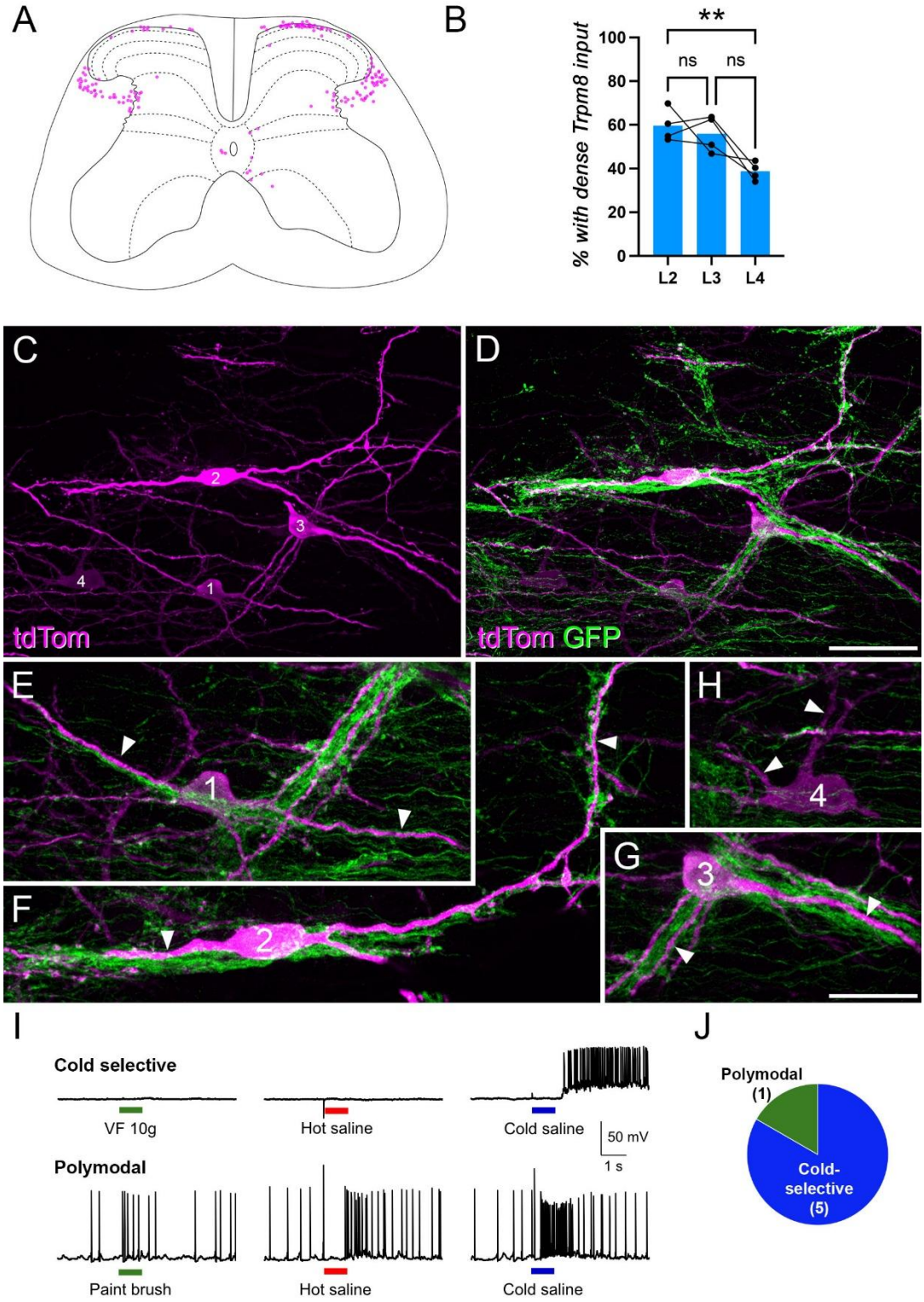

1230

1231 **Figure 5 Characterisation of Calb1-expressing projection neurons.** (**A**) The
1232 distribution of retrogradely labelled cells in 10 transverse sections from the L5 segment of
1233 one of the Calb1^{Cre} mice that had received an injection of AAV11.Cre^{ON}.tdTomato into the
1234 LPB. The right side of the plot is the side contralateral to the brain injection. (**B**) Bar chart

showing the proportion of retrogradely labelled cells in the L2, L3 and L4 segments of the Calb1^{Cre} mice injected with AAV11.Cre^{ON}.tdTomato into the LPB that received dense Trpm8 input. Repeated measures 1-way ANOVA showed a significant difference ($p = 0.048$), and post-hoc Holm-Šídák's multiple comparisons test revealed a difference only between L2 and L4 ($p = 0.0056$). (**C**) Part of a horizontal section through the L2 segment of one of the mice, showing 4 lamina I neurons (numbered 1-4) that were retrogradely labelled with tdTomato (tdTom, magenta). (**D**) The same field scanned to reveal both tdTomato and GFP (green). (**E**-**H**) detailed views of the 4 cells shown in **C**,**D**. Three of these cells (1-3) have numerous contacts from GFP-labelled axons on their dendrites (marked with arrowheads) and cell bodies. The fourth cell (4) has very few such contacts. (**I**) Recordings from one of the cold-selective cells (upper traces) and the polymodal cell (lower traces) in experiments carried out in Calb1^{Cre} mice that had received injections of AAV11.Cre^{ON}.tdTomato into the CVLM. The cell in the upper traces shows action potential firing in response to application of cold saline to the skin, but no response to application of a 10g von Frey (VF) hair or hot saline. The other cell responds to brushing of the skin with a paint brush, as well as to application of hot and cold saline. (**J**) Pie chart showing response characteristics of the 6 cells recorded in these experiments. Scale bars: (**C**,**D**) = 50 μm, (**E**-**H**) = 25 μm. **P<0.01.

Click here to enter text.

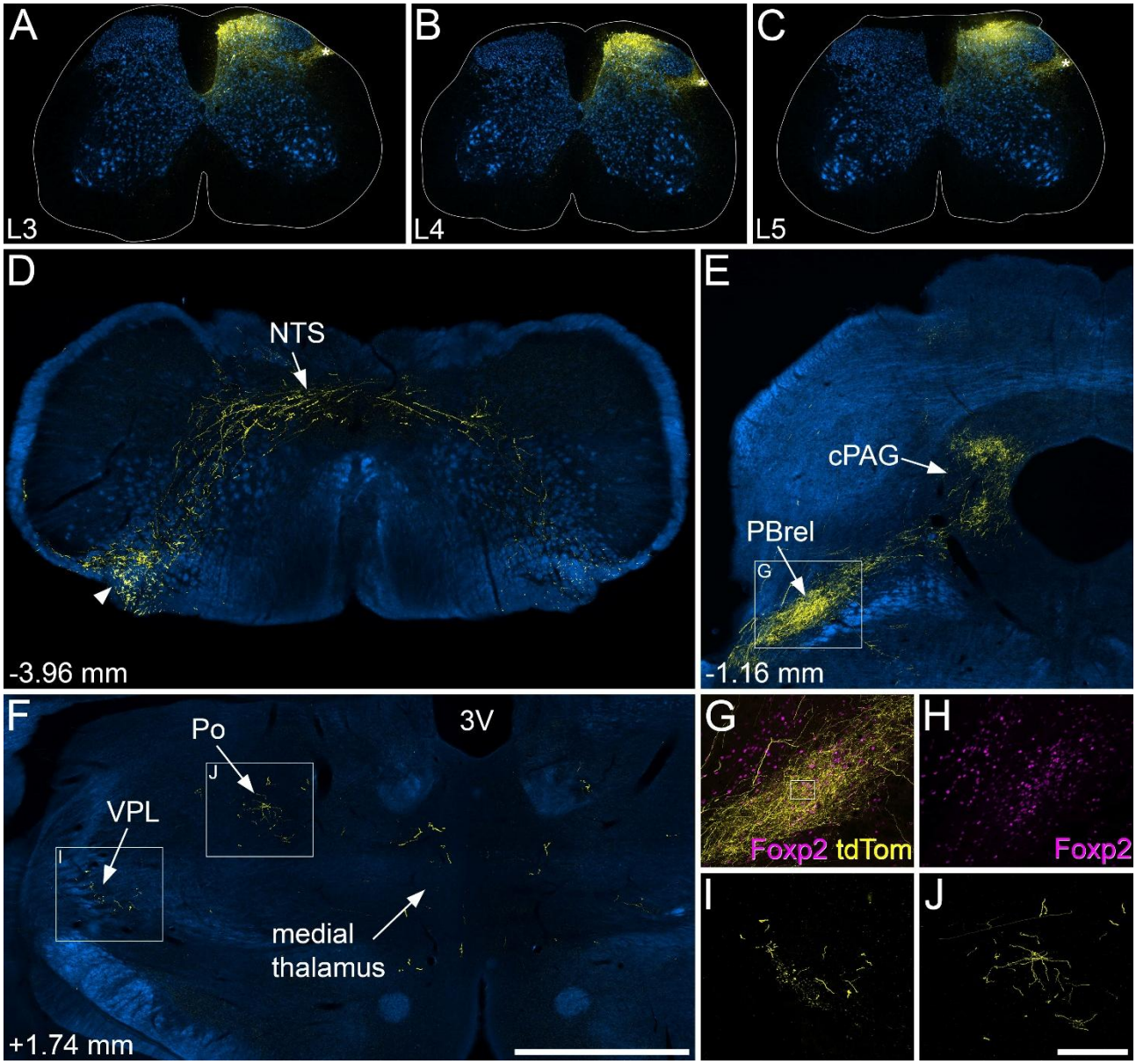

Figure 6. Anterograde tracing following injections of AAV1.Cre^{ON}.tdTomato into the medial dorsal horn of Calb1^{Cre} mice (**A**-**C**) Injection sites in the medial parts of the L3, L4 and L5 segments of one of the mice used in this part of the study. Immunostaining for tdTomato is shown in yellow and for NeuN in blue. Labelling of cell bodies is largely restricted to the medial part of the dorsal horn. There is some labelling in the lateral spinal nucleus (LSN), marked by asterisks, but this is likely to result from transport in axons of local interneurons. (**D**-**F**) Sections through selected regions of the brain immunostained to reveal tdTomato (yellow), with the corresponding dark-field images shown in blue. (**D**) At the level of the caudal medulla, the main ascending fibre bundle (arrowhead) lies in the ventrolateral region on the side contralateral to the spinal injections. Collateral axons innervate the nucleus of the solitary tract (NTS). (**E**) There is a dense projection of axons

to the rostralmost part of the lateral parabrachial area (PBrel) and the caudal part of the PAG (cPAG) on the side contralateral to the injections. (**F**) Within the diencephalon there is sparse labelling in the contralateral ventral posterolateral nucleus (VPL) and posterior nucleus (Po) as well as within the medial thalamus. (**G**,**H**) The region indicated in the box in **E** is shown at higher magnification with immunostaining for Foxp2 shown in magenta. The overlap between arborisation of tdTomato and Foxp2-positive nuclei indicates that this region is indeed PBrel. The box in (**G**) corresponds to the region shown at higher magnification in Figure 6–figure supplement 2F. (**I**, **J**) show higher magnification views of tdTomato-positive axons in the VPL and Po, respectively, corresponding to the boxes in (**F**). Numbers in **D**-**F** show approximate rostrocaudal locations in relation to the interaural line. Images in **A**-**E**, **G**-**H** are from animal #8, and those in **F**, **I**, **J** are from animal #7 in Table 1. Scale bars: (**A**-**F**) = 1 mm, (**G**-**J**) = 200 μm.

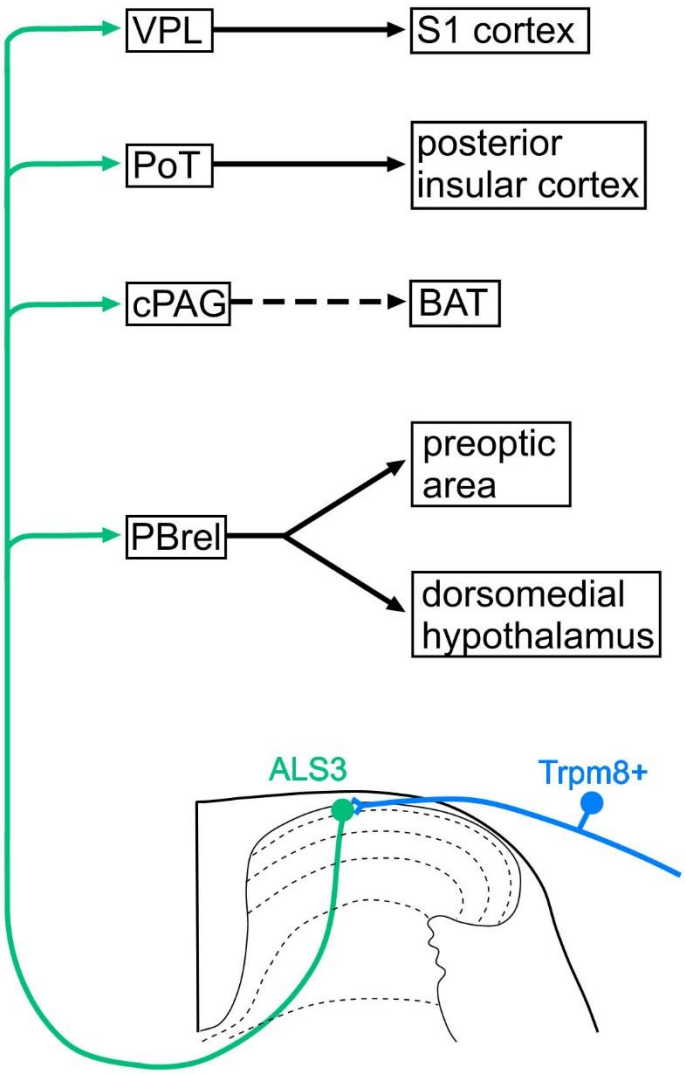

Figure 7. Proposed circuits involving cold-selective lamina I ALS neurons Our results suggest that cold-selective lamina I projection neurons, which belong to the ALS3 cluster[13] project, among other sites, to PBrel, the caudal part of the PAG (cPAG) and the ventral posterolateral nucleus of the thalamus (VPL). Cold-responsive cells in PBrel innervate the preoptic area and dorsomedial hypothalamus, which are integral components of circuits that underlie cold defence. The cPAG can indirectly activate brown adipose tissue (BAT) metabolism, also contributing to cold defence. The projection to PoT and VPL, through their connections to the posterior insular and primary somatosensory (S1) cortices, presumably underlies conscious perception of cold stimuli applied to the skin. Although we show a single ALS3 neuron projecting to different brain regions, it is possible that branches to different brain nuclei originate from specific subsets of ALS3 neurons. Note

Click here to enter text.

1292 that in addition to the direct (monosynaptic) input from Trpm8-expressing primary afferents
1293 to ALS3 neurons, there may also be indirect (e.g. polysynaptic) inputs arriving via
1294 excitatory interneurons.

1295

1296 **FIGURE SUPPLEMENTS**

1297

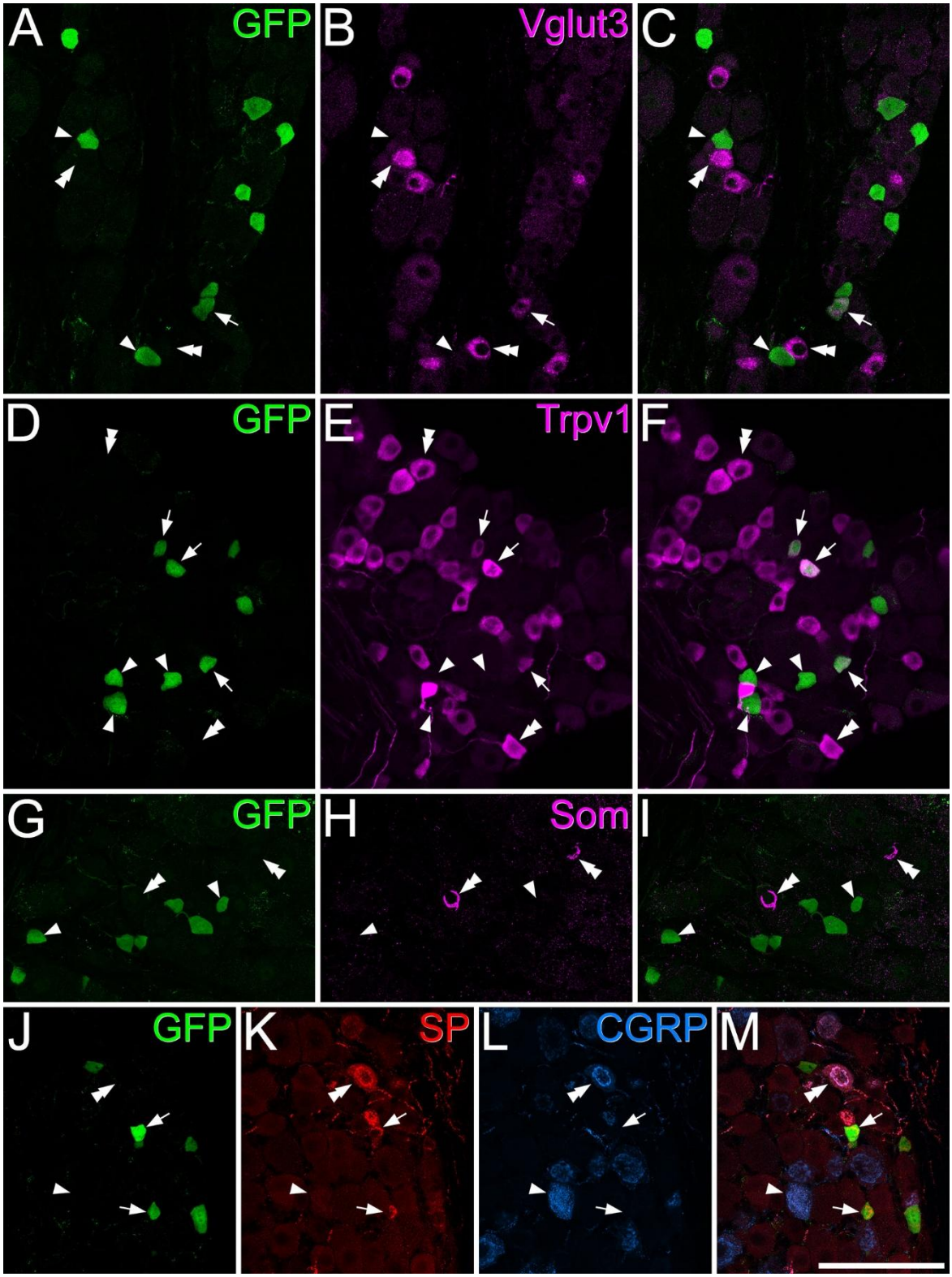

1298

1299 **Figure 1–figure supplement 1. Immunohistochemical characterisation of GFP-**
1300 **expressing somata in dorsal root ganglia of Trpm8^{Flp};RCE:FRT mice.** In each set of
1301 images GFP immunoreactivity is shown in green and other types of immunoreactivity in

1302 magenta, red or blue. (**A**-**C**) GFP and Vglut3 are present in largely separate populations,
1303 although some cells contain both proteins (one cell in this field, marked with an arrow).
1304 Two cells containing only GFP are indicated with arrowheads, and two cells containing
1305 only Vglut3 with double arrowheads. (**D**-**F**) There is a greater degree of overlap between
1306 GFP and Trpv1, and three double-labelled cells are shown with arrows. Some cells with
1307 only GFP or Trpv1 are indicated with single and double arrowheads, respectively. (**G**-**I**)
1308 GFP and somatostatin (Som) are found in separate populations, and some labelled cells
1309 are marked with single and double arrowheads, respectively. Note that somatostatin is
1310 seen as a partial ring around the nucleus in cells that express the peptide. (**J**-**M**) GFP cells
1311 often contain substance P (SP) but lack calcitonin gene-related peptide (CGRP), and 2 of
1312 these are marked with arrows. A single and double arrowhead mark cells with CGRP only
1313 and with both SP and CGRP, respectively. Scale bar: (**A**-**M**) = 100 μm.
1314

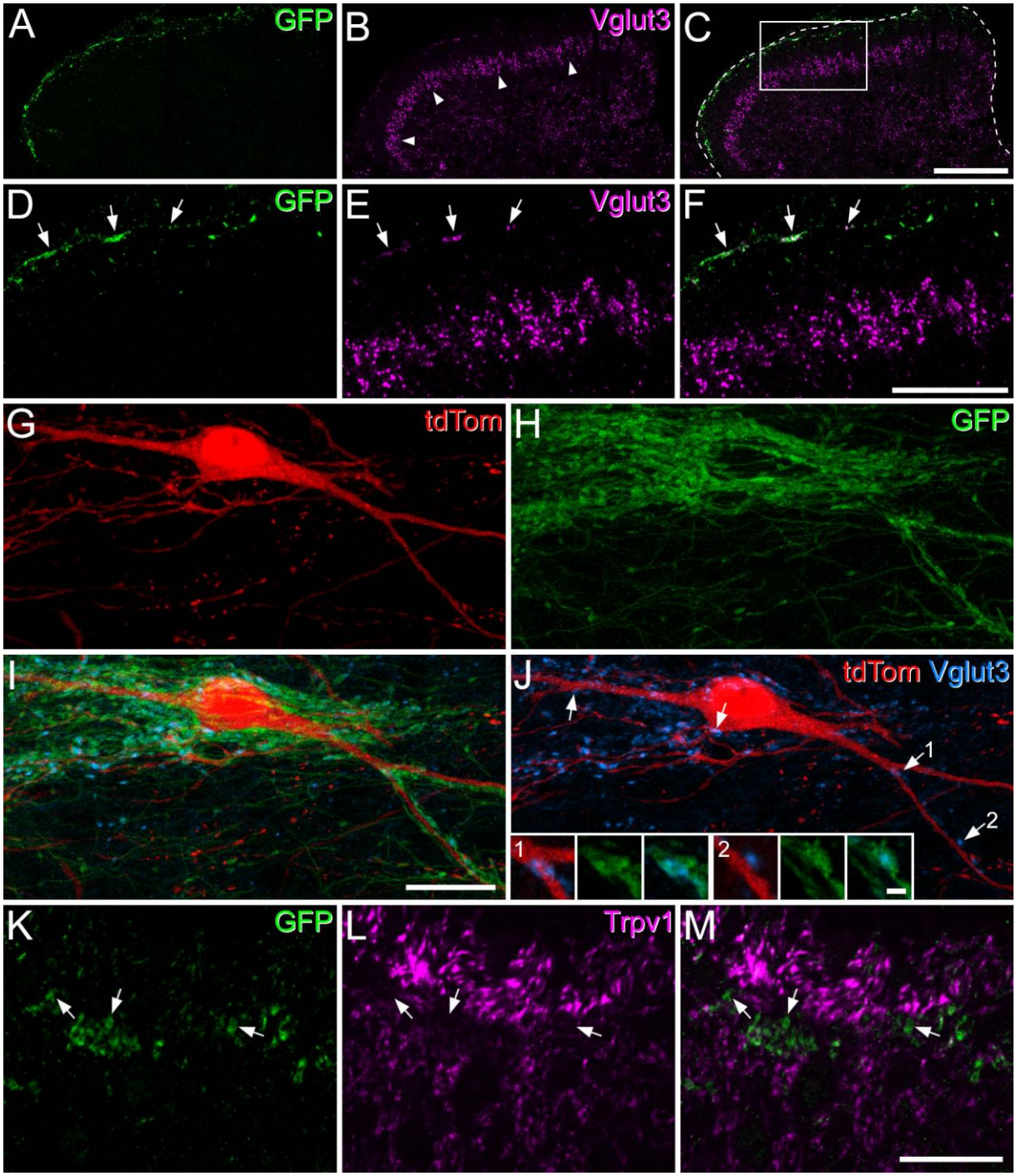

Figure 2–figure supplement 1. Expression of Vglut3 and lack of detectable Trpv1 in the central terminals of Trpm8 afferents. (**A-C**) A low magnification confocal image from a transverse section of the L2 segment in a Trpm8^{Flp};RCE:FRT mouse immunostained for GFP (green) and Vglut3 (magenta). GFP-labelled axons are restricted to lamina I, while a dense band of Vglut3-immunoreactive terminals in the inner part of lamina II (marked with arrowheads) corresponds to the central terminals of C low-threshold mechanoreceptors. The dashed line in C shows the outline of the dorsal horn and the box indicates the area shown in (**D-F**). (**D-F**) At higher magnification a few Vglut3 profiles are also seen in lamina

1324 I (arrows) and these co-express GFP. (**G**-**J**) A horizontal section through lamina I from a
1325 Phox2a::Cre;Ai9;Trpm8^{Flp};RCE:FRT mouse immunostained to reveal tdTomato (tdTom,
1326 red), GFP (green) and Vglut3 (blue). This field includes a tdTomato labelled projection
1327 neuron that receives numerous contacts from GFP-labelled axons. Some of these are also
1328 immunoreactive for Vglut3 and these are seen more clearly (some marked with arrows)
1329 when only tdTomato and Vglut3 are revealed (**J**). The insets in J show two of these Vglut3
1330 profiles (those marked with arrows numbered 1 and 2) contacting dendrites of the
1331 projection neuron in limited z-projections (2 optical sections at 0.5 µm z-spacing). In these
1332 images the coexpression of Vglut3 (blue) and GFP (green) is clearly visible. (**K**-**M**) A
1333 transverse section through lamina I from a Trpm8^{Flp};RCE:FRT mouse immunostained to
1334 reveal GFP (green) and Trpv1 (magenta). Although numerous Trpv1-immunoreactive
1335 profiles are visible, labelling for Trpv1 is generally not detected in the Trpm8 afferents,
1336 which express GFP. Scale bars: (**A**-**C**) = 100 µm, (**D**-**F**) = 50 µm, (**G**-**J**) = 50 µm, (**K**-**M**) =
1337 20 µm, (insets in **J**) = 2 µm.
1338
1339

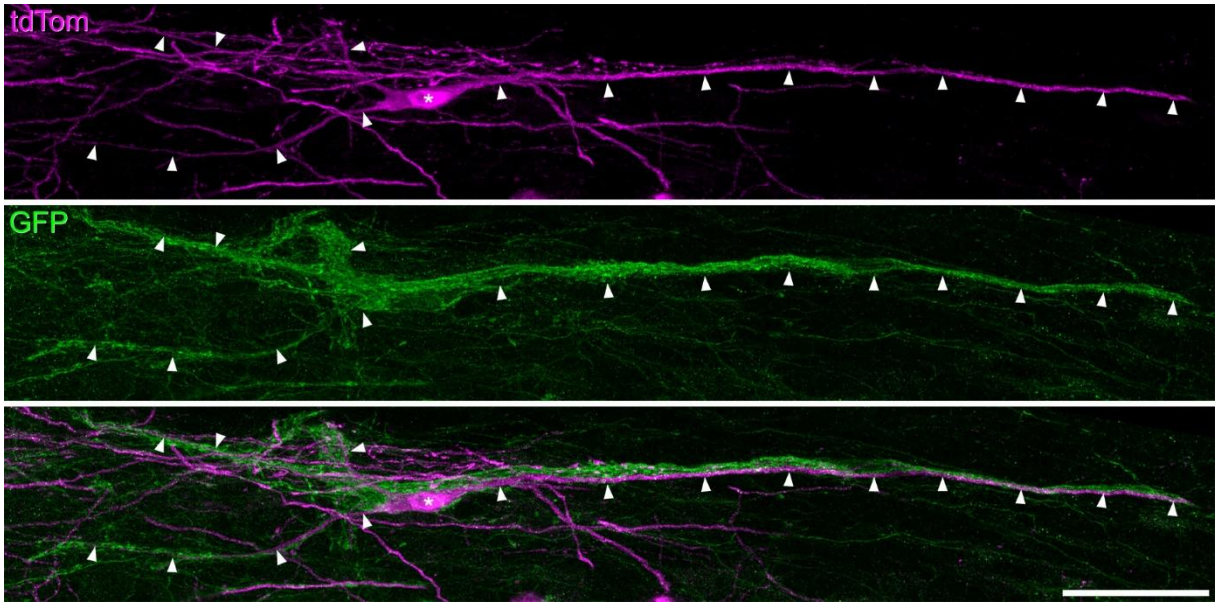

Figure 3–figure supplement 1. The relationship between tdTomato and GFP labelling for the cell illustrated in Figure 3. The top pane shows immunostaining for tdTomato (tdTom, magenta) in a horizontal section through lamina I from a Phox2a::Cre;Ai9;Trpm8^{Flp};RCE:FRT mouse. The tdTomato-labelled projection neuron illustrated in Figure 3 is visible. The soma is marked with an asterisk and parts of the dendritic tree with arrowheads. The cell body and dendrites are associated with dense bundles of GFP-labelled axons. Scale bar = 50 μm.

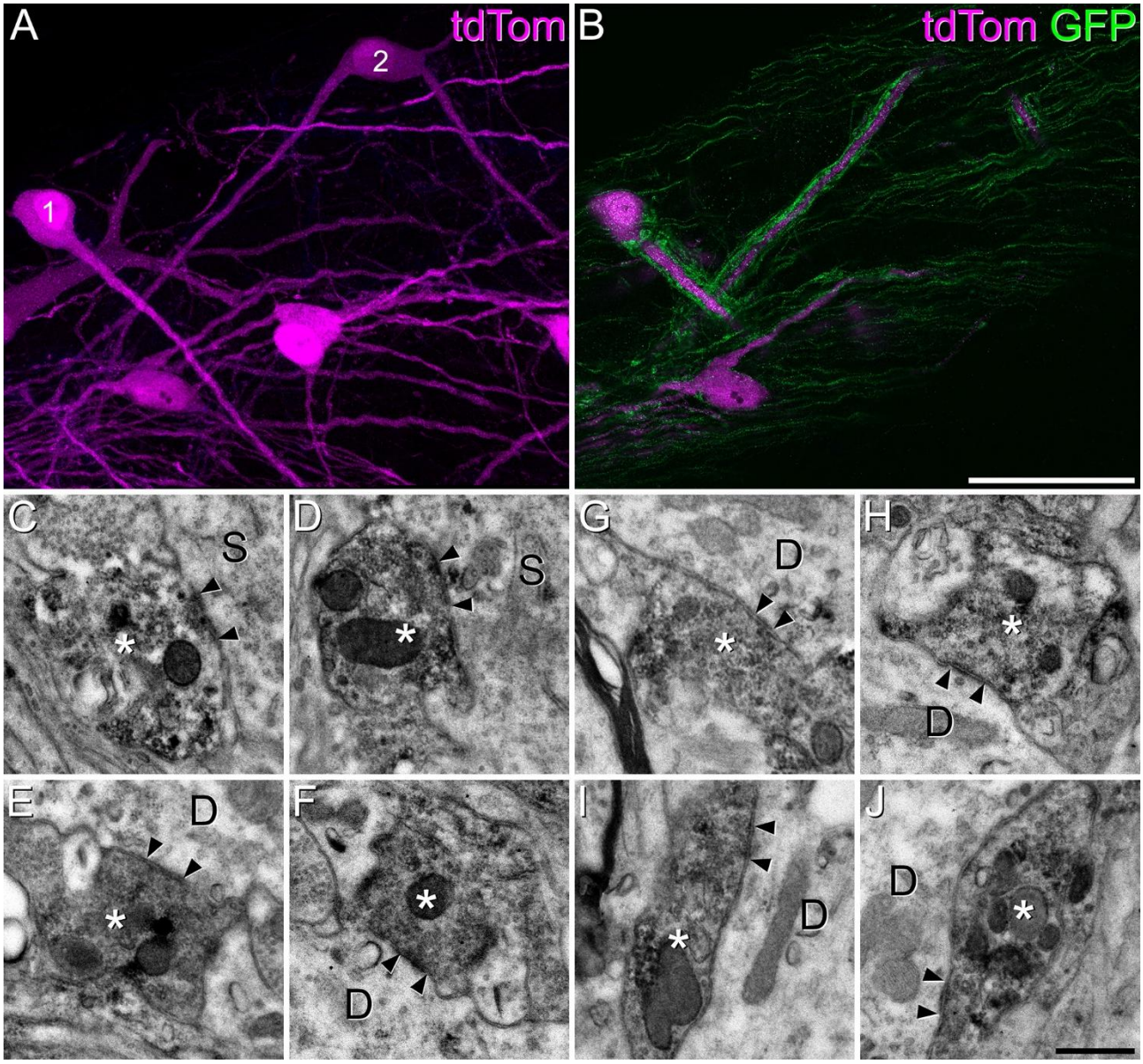

Figure 3–figure supplement 2. Confocal and electron microscope images of two Trpm8-innervated cells examined with the combined method in spinal cord sections from a Phox2a::Cre;Ai9;Trpm8^{Flp};RCE:FRT mouse. (**A**) Projected confocal z-stack showing parts of the two cells (numbered 1, 2) labelled with tdTomato (magenta) in a horizontal section. (**B**) a single optical section from the same confocal z-stack showing the association between axons labelled with GFP (green) and the cell body of cell 1 and dendrites of both cells. (**C-J**) Examples of synapses between the GFP-containing boutons, which are labelled with an immunoperoxidase method, and (unlabelled) dendrites (D) or soma (S) of the tdTomato-positive projection neurons. **C-F** show synapses on cell 1, and **G-J** those on cell 2. Presumed synaptic active zones (marked by arrowheads) can be recognised by the presence of vesicles on the presynaptic side and darkening of the

1364 membrane. However, these synapses do not show prominent postsynaptic densities.

1365 Scale bars: (**A**,**B**) = 50 µm, (**C**-**J**) = 500 nm.

1366

Click here to enter text.

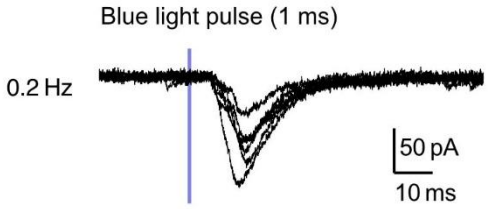

1367

1368 **Figure 3–figure supplement 3. Optogenetic evidence for possible polysynaptic input**
1369 **from Trpm8 afferents to a lamina I ALS cell with dense Trpm8 input** An example trace
1370 of an ALS cell with monosynaptic, and possibly also polysynaptic, inputs. Note that the
1371 delayed EPSCs exhibit latency jitter.

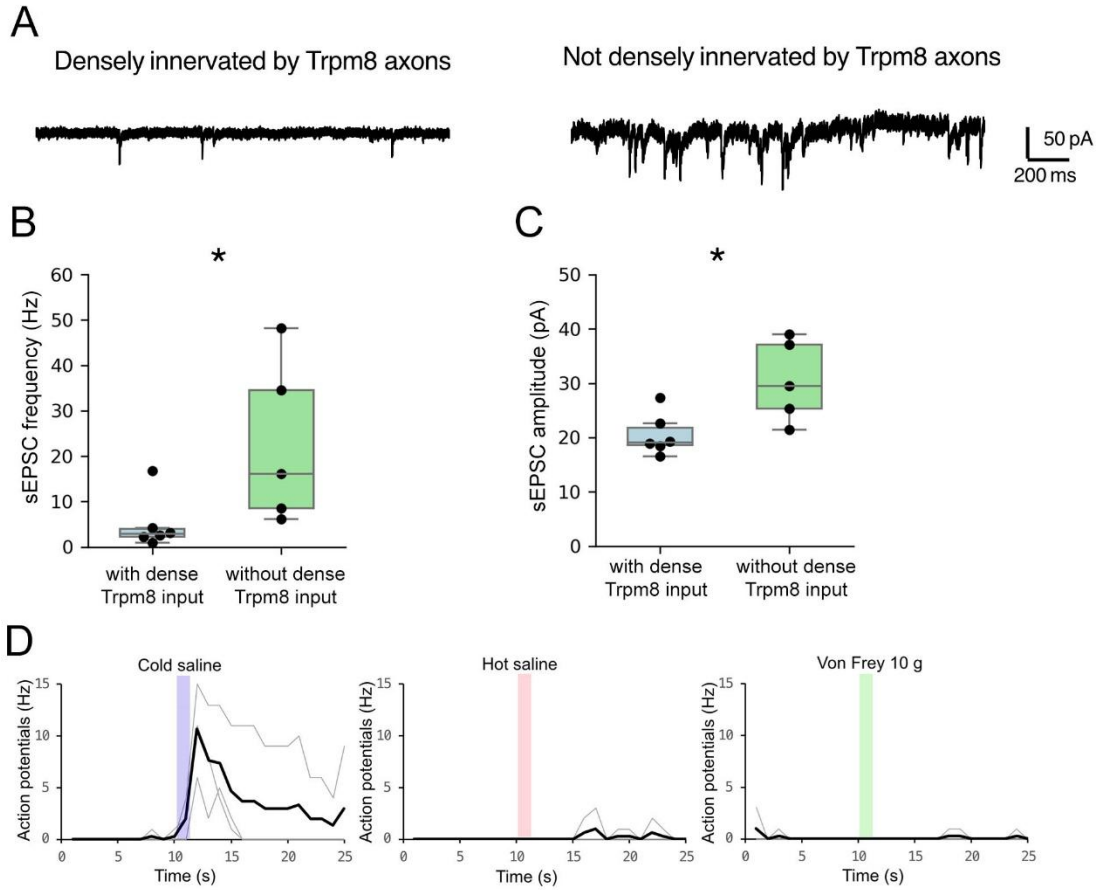

Figure 4–Figure supplement 1. Characteristics of spontaneous EPSCs in cold-selective and other lamina I ALS cells. (**A**) Representative traces from an ALS neuron with dense Trpm8 input (left) and an ALS neuron without dense Trpm8 input (right). (**B**,**C**) Quantification of sEPSC frequency (**B**) and amplitude (**C**) of ALS neurons. Box plots are median and interquartile range with symbols representing data points from individual ALS neurons (with dense Trpm8 input: n=6, without dense Trpm8 input: n=5; * indicates $p < 0.05$, Mann-Whitney U test). (**D**) Overlay of the firing time course of 3 cold-selective cells in response to cold, heat and mechanical stimulation. Note that action potentials frequency was determined from counts in 1 sec bins. Individual traces shown in grey and averages in black.

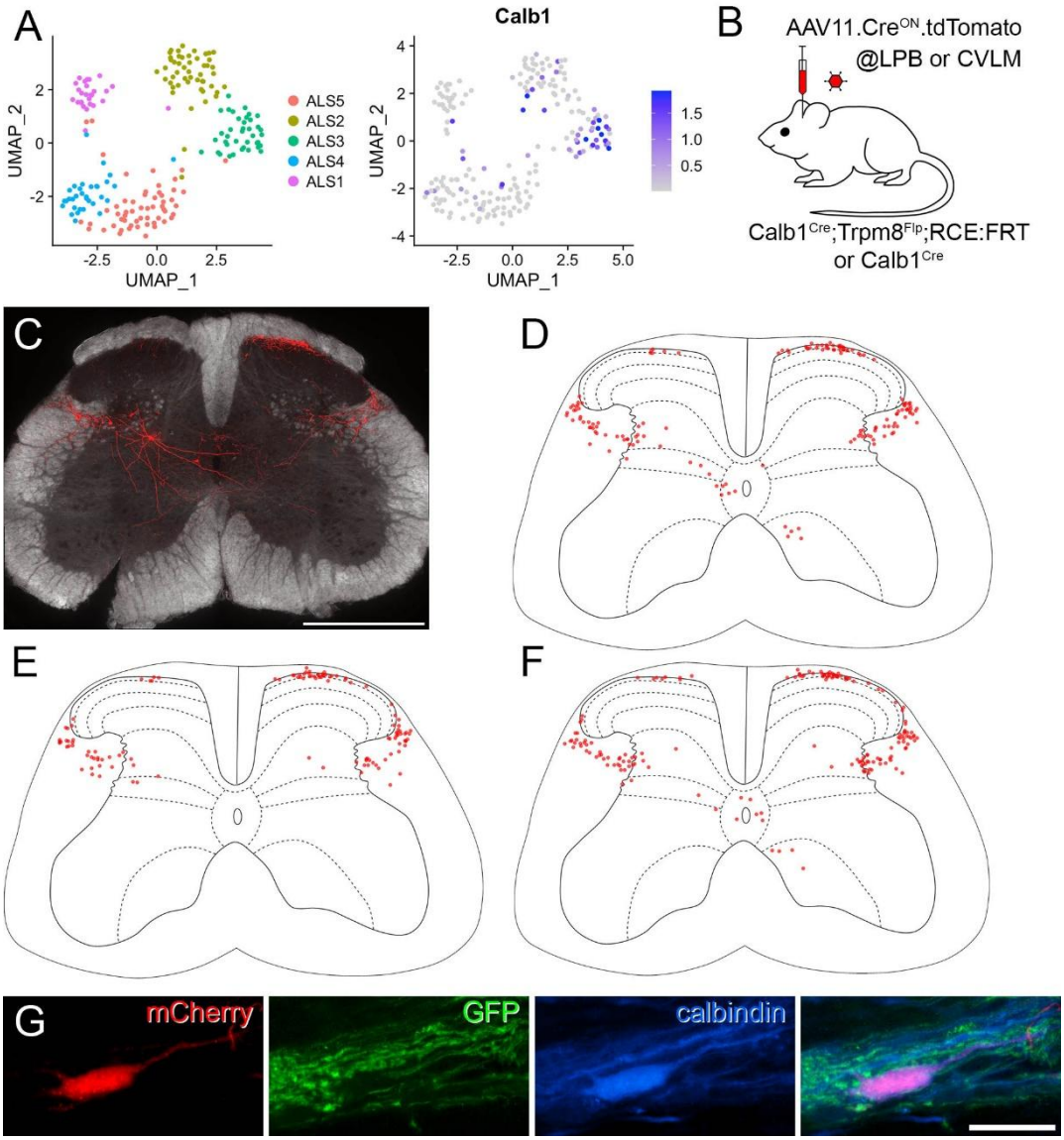

Figure 5–figure supplement 1. **Further characterisation of Calb1-expressing projection neurons.** (**A**) UMAP plot showing the distribution of cells in the ALS1-5 clusters, together with a plot for expression of Calb1. Note the presence of many Calb1-positive cells in the ALS3 cluster. (**B**) The experimental approach used to generate data presented in this figure and in Figure 5. (**C**) An example of a section through the L5 segment from a Calb1^{Cre} mouse injected with AAV11.Cre^{ON}.tdTomato in the LPB. Expression of tdTomato (red) is superimposed on a dark field image. (**D-F**) The distribution of retrogradely labelled cells in 9 (**D**,**F**) or 8 (**E**) transverse sections from the L5 segments of the remaining 3 Calb1^{Cre} mice injected with AAV11.Cre^{ON}.tdTomato in the LPB. The labelling for the other mouse is shown in Figure 5A. (**G**) Horizontal section through lamina I from the L4 segment of a Trpm8^{Flp};RCE:FRT mouse that had been injected with AAV9.mCherry into the LPB. The section has been immunoreacted to reveal mCherry

1397 (red), GFP (green) and calbindin (blue). A mCherry-positive lamina I neuron that is
1398 surrounded by GFP axons shows strong calbindin-immunoreactivity. Scale bar: (**C**) = 500
1399 µm, (**G**) = 20 µm.
1400

Click here to enter text.

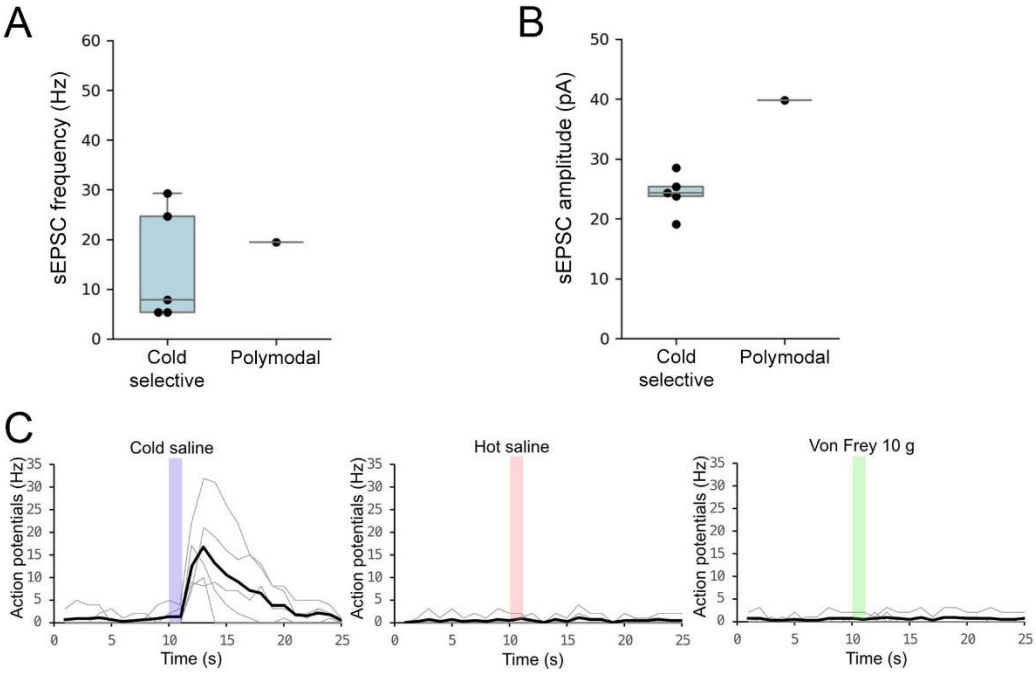

Figure 5–figure supplement 2. **Electrophysiological characterisation of Calb1-expressing projection neurons.** (**A, B**) sEPSC frequencies and amplitudes for the 5 cold-selective cells and the 1 polymodal cell recorded in Calb1^{Cre} mice injected with AAV11.Cre^{ON}.tdTomato in the CVLM. Note that although 2 of the cold-selective cells in this sample had relatively high sEPSC frequencies, when data from these cells were pooled with those reported for other sample of cold-selective cells (shown in Figure 4–Figure supplement 1) and compared with the polymodal cells shown in that Figure supplement, there was still a significant difference for both sEPSC frequency ($p = 0.037$) and amplitude ($p = 0.015$) (Mann-Whitney U test). (**C**) Overlay of the firing time course of 5 cold-selective cells in response to cold, heat and mechanical stimulation. Note that action potentials frequency was determined from counts in 1 sec bins. Individual traces shown in grey and averages in black.

Click here to enter text.

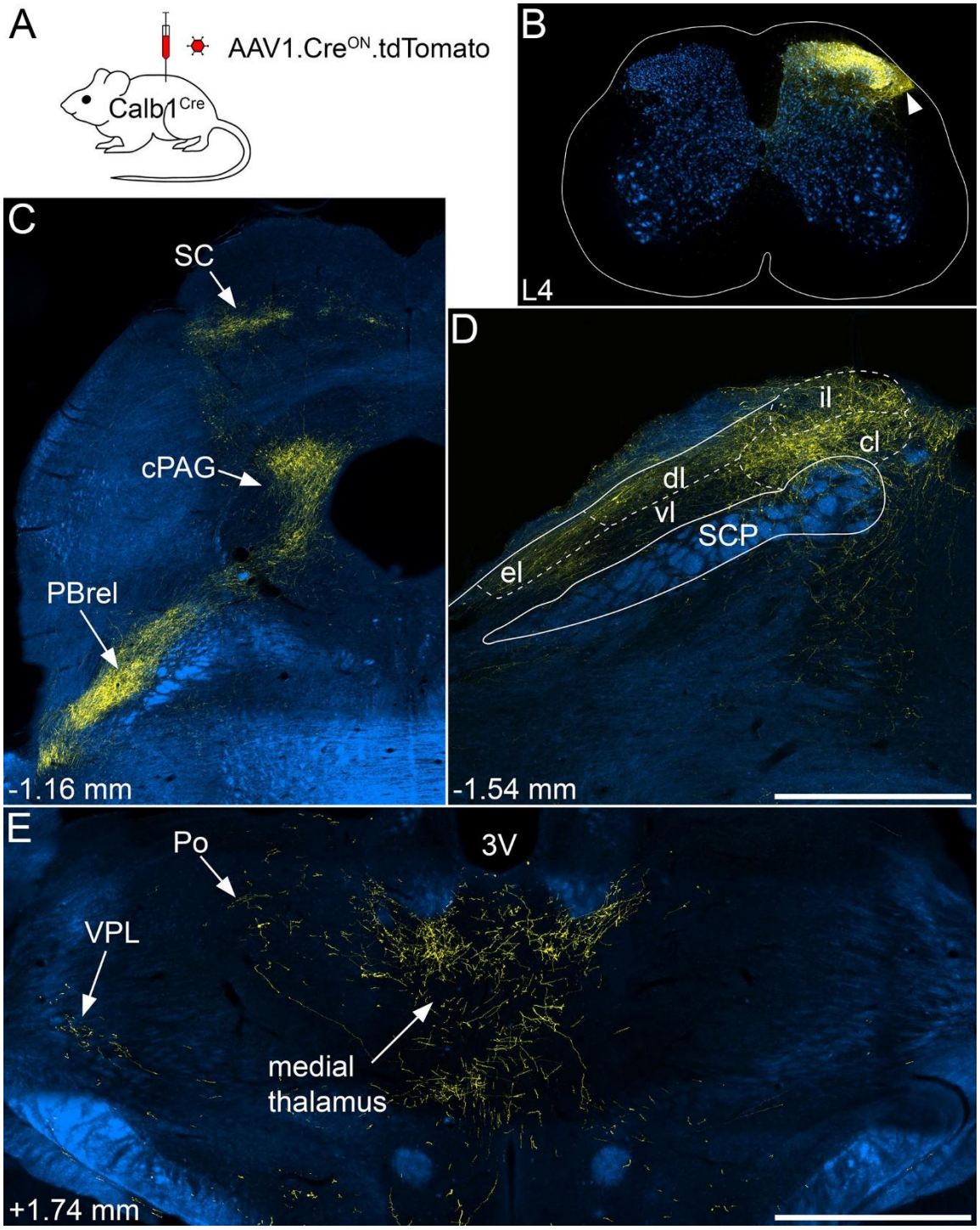

Figure 6–figure supplement 1. Anterograde labelling following injections of AAV1.Cre^{ON}.tdTomato into the central part of the spinal dorsal horn of Calb1^{Cre} mice. (**A**) The experimental approach used to generate data for Figure 6 and for Figure 6–figure supplements 1-3. Intraspinal injections were made into either the L3 or the L3, L4 and L5 segments, and were targeted on either the central or medial part of the dorsal horn. (**B**) Example of an injection into the central part of the L4 segment of a Calb1^{Cre} mouse. Immunostaining for tdTomato is shown in yellow and for NeuN in blue. There is extensive

tdTomato labelling throughout most of the dorsal horn, and this extends into the lateral spinal nucleus (arrowhead), which contains tdTomato-labelled cell bodies. (**C**-**E**) Sections through selected regions of the brain have been immunostained to reveal tdTomato (yellow), and these are shown on corresponding dark-field images (blue). (**C**) There is strong labelling in the rostralmost part of the contralateral LPB, corresponding to the PBrel, as well as in the caudal PAG (cPAG). Unlike the pattern seen with injections restricted to the medial dorsal horn, there is also strong labelling in the contralateral superior colliculus (SC). (**D**) At a slightly more caudal level there is axonal labelling in several subnuclei of the contralateral LPB, including external lateral (el), dorsolateral (dl), central lateral (cl) and internal lateral (il), but not ventrolateral (vl). The location of the superior cerebellar peduncle (SCP) is indicated. (**E**) Within the diencephalon there is sparse axonal labelling in contralateral VPL and posterior (Po) thalamic nuclei, as seen following medial injections. However, there is also dense labelling in the medial thalamus, which was not seen with medial injections. Numbers in **C**-**E** show approximate rostrocaudal locations in relation to the interaural line. All images are from animal #2 in Table 1. Scale bars: (**B**,**C**,**E**) = 1 mm, (**D**) = 500 μm.

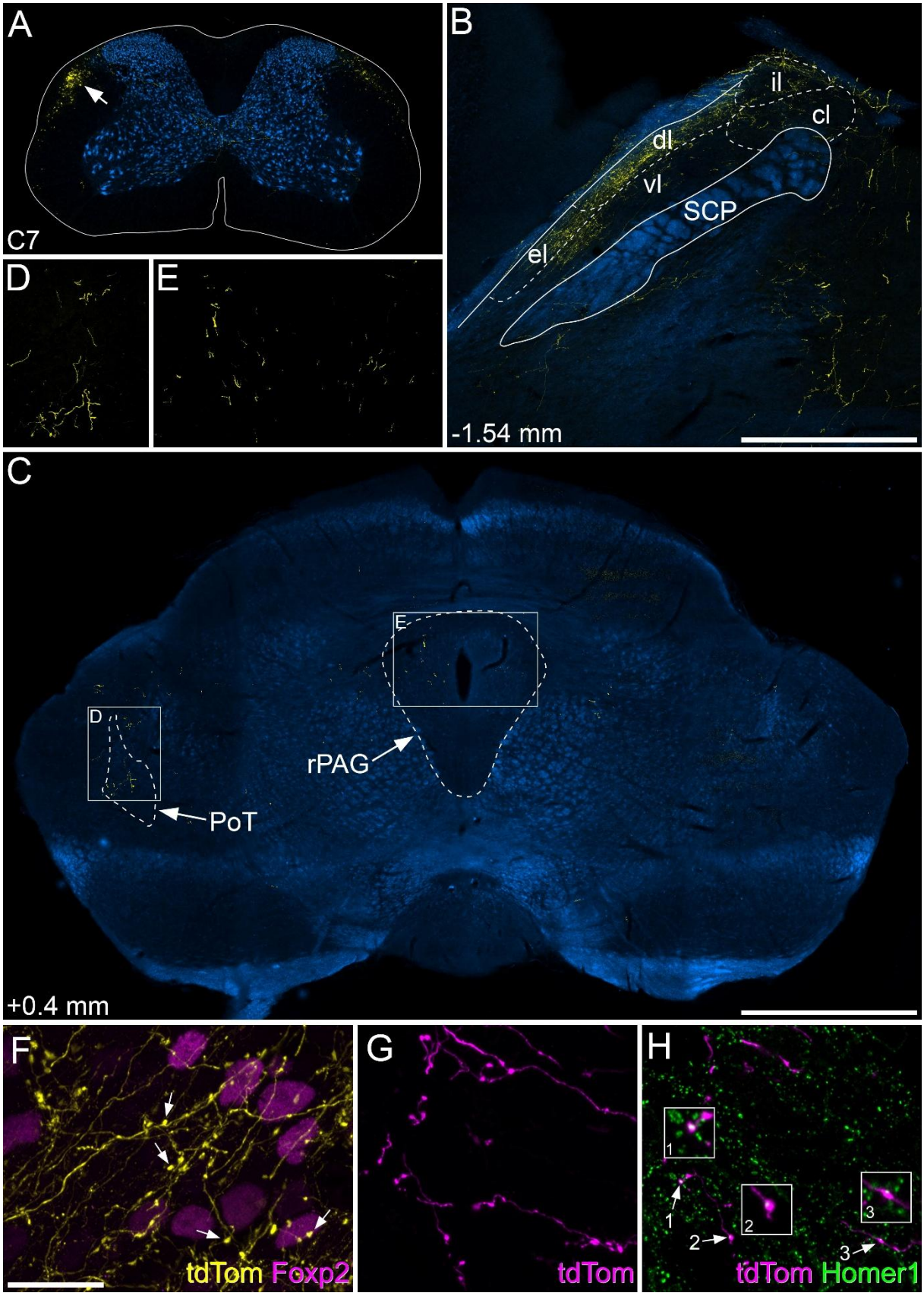

Figure 6–figure supplement 2. Anterograde labelling following injections of AAV.Cre^{ON}.tdTomato into the medial dorsal horn of Calb1^{Cre} mice. (**A**) A section through the C7 segment of a mouse that received injections into L3, L4 and L5 segments.

Click here to enter text.

1444 Immunostaining for tdTomato is shown in yellow and for NeuN in blue. There is a bundle of
1445 axons (arrow) in the contralateral dorsolateral white matter, with a much more weakly
1446 stained bundle in the same location on the opposite side. A few collateral branches are
1447 present in the deep dorsal horn and the area around the central canal. (**B**,**C**) Sections
1448 through selected regions of the brain have been immunostained to reveal tdTomato
1449 (yellow), and this is shown on corresponding dark-field images (blue). (**B**) At this level of
1450 the contralateral LPB, there is axonal labelling in the external lateral (el) and dorsolateral
1451 (dl) subnuclei, with very little labelling in ventrolateral (vl), central lateral (cl) or internal
1452 lateral (il). The location of the superior cerebellar peduncle (SCP) is indicated. (**C**) At a
1453 level corresponding to ~ 0.4 mm rostral to the interaural line there is very sparse axonal
1454 labelling in the posterior triangular nucleus of the thalamus (PoT) and in the rostral PAG
1455 (rPAG) on the side contralateral to the spinal injection. This is shown at higher
1456 magnification in (**D**) and (**E**), which correspond to the boxes in (**C**). (**F**) shows a maximum
1457 intensity projection of a z-series of 39 optical sections (0.5 µm z-separation) corresponding
1458 to part of the image shown in Figure 6G. Several varicosities, which probably correspond
1459 to synaptic boutons, are visible, and some are indicated with arrows. (**G**, **H**) High
1460 magnification views of anterogradely labelled axon terminals in the PBrel of a mouse that
1461 received injections into the L3, L4 and L5 segments. Immunostaining for tdTomato is
1462 shown in magenta and for Homer1 in green. The image in (**G**) is a maximum intensity
1463 projection from 23 optical sections at 0.5 µm z-separation, showing labelled axons with
1464 varicosities. (H) shows a projection of 3 optical sections (0.5 µm z-separation). Three of
1465 the varicosities in this field (arrows) are associated with Homer1 puncta and these are
1466 shown at higher magnification in insets. Note that the colour used to represent tdTomato
1467 has been altered to display the relation of Homer1 puncta to tdTomato varicosities.
1468 Numbers in **B** and **C** show approximate rostrocaudal locations in relation to the interaural
1469 line. Images in **A** and **C**-**E** are from animal #7, those in **B** and **F** are from animal # 8, and
1470 those in **G** and **H** are from animal #10 in Table 1. Scale bars: (**A**,**C**) = 1 mm, (**B**,**D**,**E**) = 500
1471 µm, (**F**-**H**) = 20 µm.
1472

1473

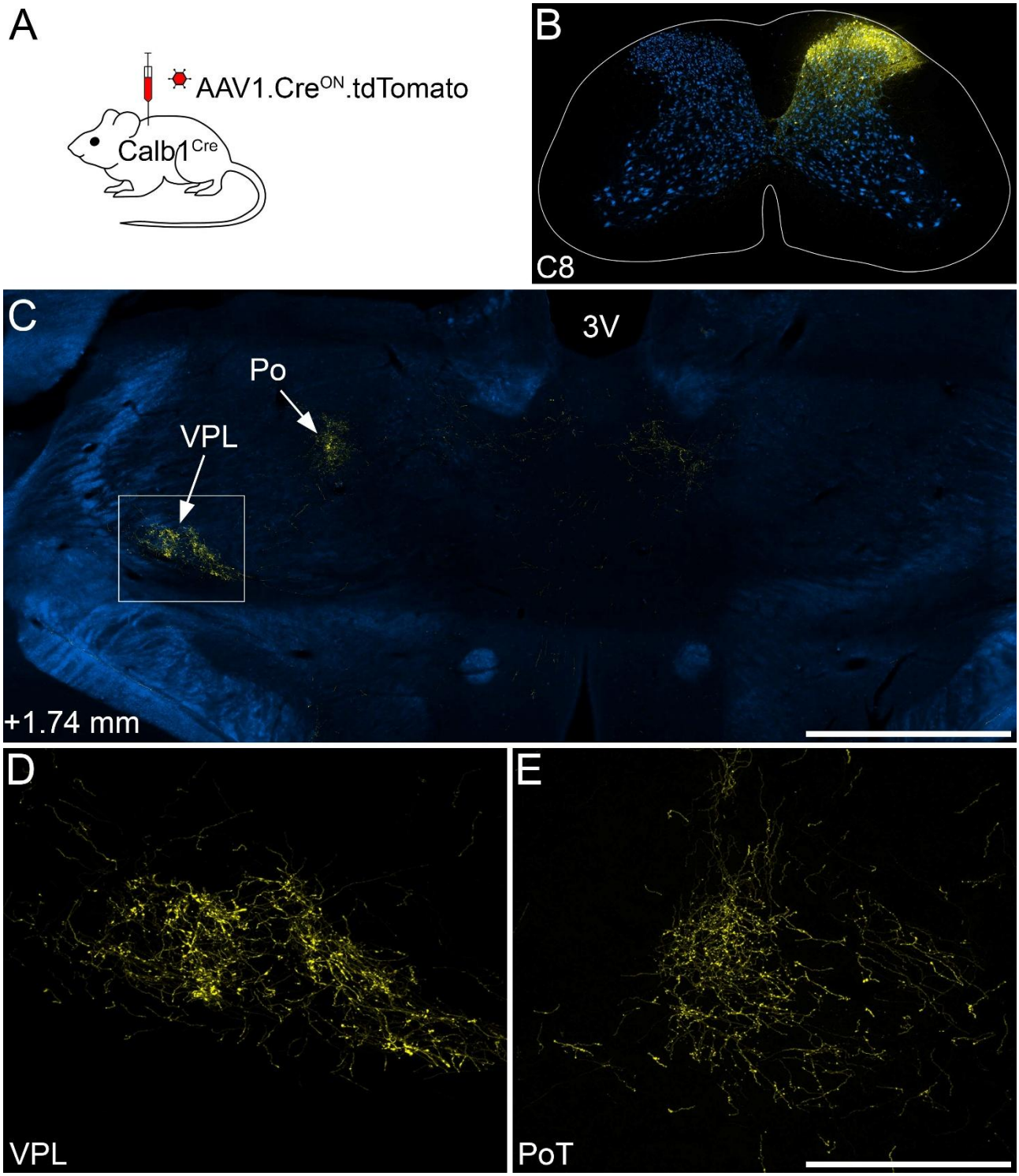

Figure 6–figure supplement 3. Anterograde labelling following injections of AAV.Cre^{ON}.tdTomato into the cervical dorsal horn of Calb1^{Cre} mice (**A**) The experimental approach used to generate data for this figure. Injections were made into the cervical enlargement. (**B**) Injection site in the C8 segment. Immunostaining for tdTomato is shown in yellow and for NeuN in blue. (**C**) A section through the diencephalon scanned to reveal tdTomato (yellow) and dark-field illumination (blue) shows dense tdTomato labelling

in the VPL and Po thalamic nuclei. The region in the box is shown at higher magnification in **D**. (**D**) Dense tdTomato labelling can be seen in the VPL. (**E**) At a more caudal level, there is also dense tdTomato labelling in the PoT nucleus of thalamus. The number in C shows the approximate location in relation to the interaural line. All images are from animal #14 in Table 1. Scale bars: (**B**,**C**) = 1 mm, (**D**,**E**) = 250 µm.

Click here to enter text.

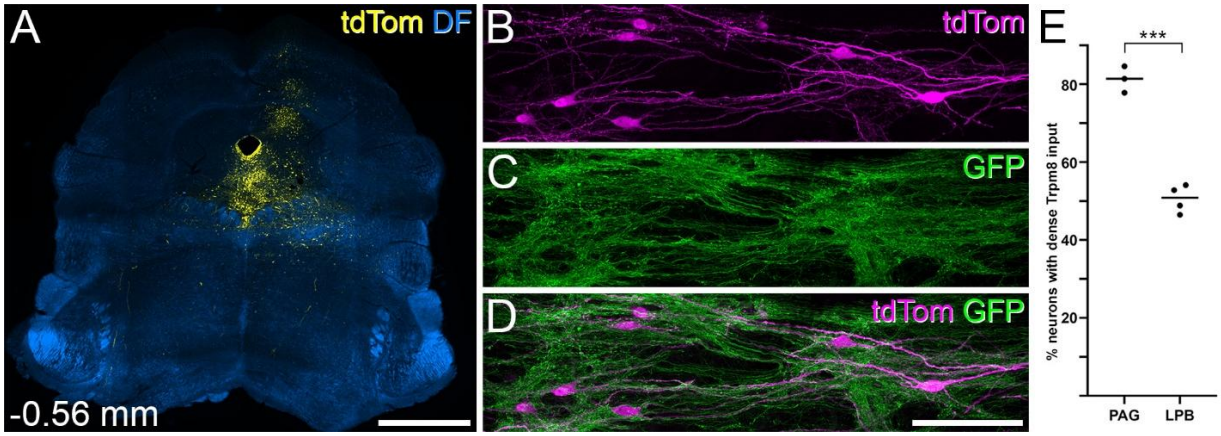

Figure 6–figure supplement 4. Retrograde labelling of Calb1-expressing ALS neurons from PAG. (**A**) TdTomato labelling at the site of injection of AAV11.Cre^{ON}.tdTomato in one of the 3 Calb1^{Cre};Trpm8^{Flp};RCE:FRT mice used in this part of the study. Note that this will not reveal the precise location of the injection, because only nearby Calb1-expressing cells will be labelled. (**B**-**D**) Labelling for tdTomato (tdTom) and GFP in a horizontal section through lamina I from the case illustrated in (**A**). Several tdTom-positive neurons are visible in this field, and all of them are densely coated with GFP-labelled (Trpm8-positive) axons. (**E**) Histogram showing the percentages of retrogradely labelled neurons in the L2-L4 segments that were densely coated with Trpm8-positive axons in this set of experiments (PAG), compared with the corresponding values from the 4 cases in which AAV11.Cre^{ON}.tdTomato was injected into the LPB. There was a highly significant difference between the percentages between the two injection sites ($p < 0.0001$, unpaired t-test with Welch's correction). Scale bars: (**A**) = 1 mm, (**B**-**D**) = 100 µm.

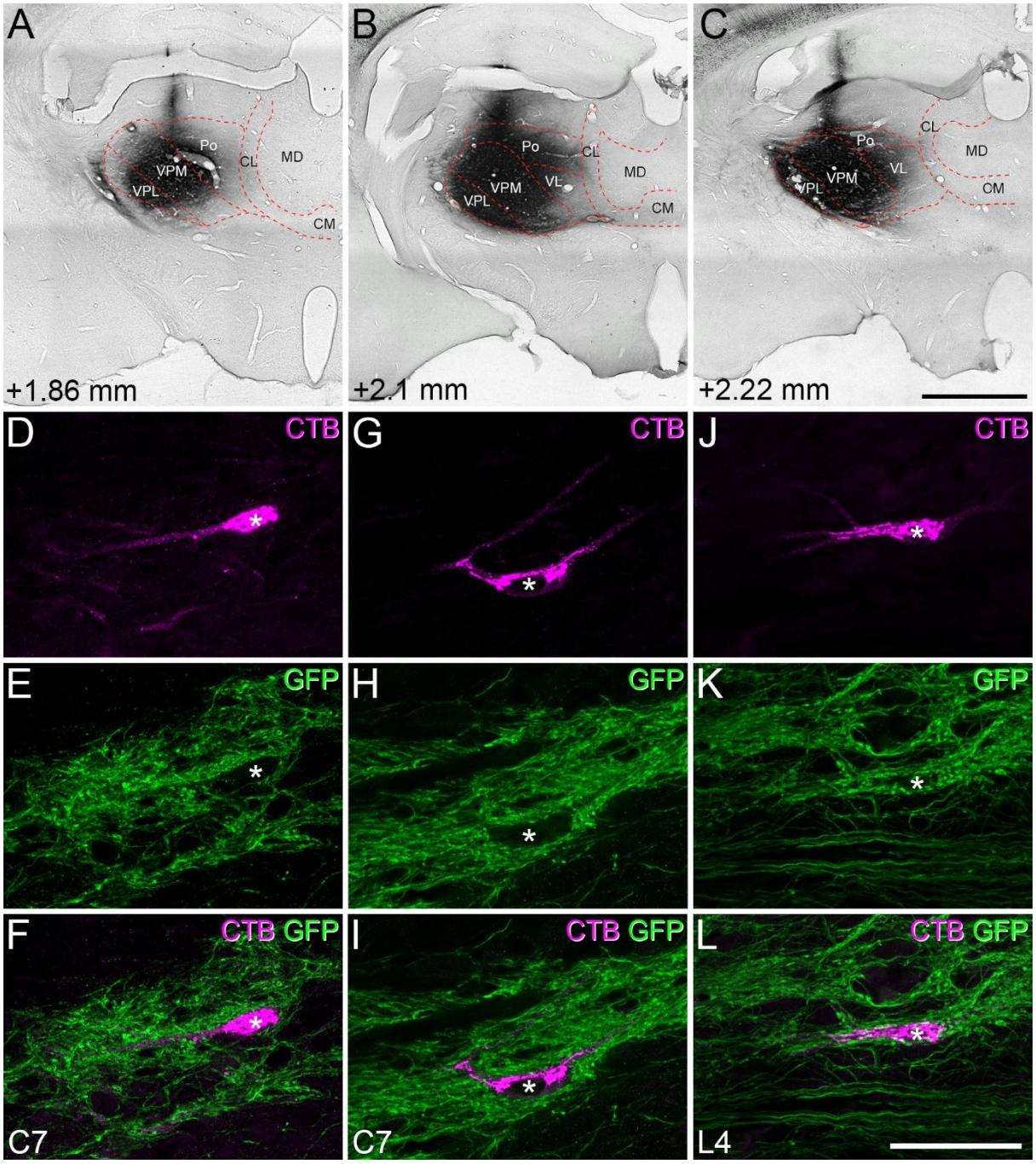

Figure 6–figure supplement 5. Identification of spinothalamic lamina I neurons with dense Trpm8 input. (**A**-**C**) CTB injection sites in the 3 experiments. In each case there is dense labelling in the ventral posterolateral (VPL) and ventral posteromedial (VPM) nuclei, together with some labelling in the posterior (Po) nucleus, and in two cases also in the ventrolateral (VL) nucleus. Note the lack of labelling in medial thalamic nuclei (centrolateral, CL; centromedial, CM; mediodorsal, MD). Numbers show approximate rostrocaudal locations in relation to the interaural line. (**D**-**I**) Examples of retrogradely labelled (CTB-positive) lamina I neurons (marked with asterisks) that are associated with numerous GFP-labelled (Trpm8-expressing) axons in horizontal sections through the C7

segments in the experiments illustrated in **A** and **B**. (**J**-**L**) In the experiment illustrated in **C**, we also identified 5 CTB-labelled cells in the L4 segment, and one of these, which is associated with numerous GFP-labelled boutons, is shown here (asterisk). Note that we also found CTB-labelled cells associated with numerous GFP-positive boutons in the C7 segment in this experiment. In each case, the images are shown below the injection site from the corresponding experiment. Scale bars: (**A**-**C**) = 1 mm, (**D**-**L**) = 50 μm.

Click here to enter text.

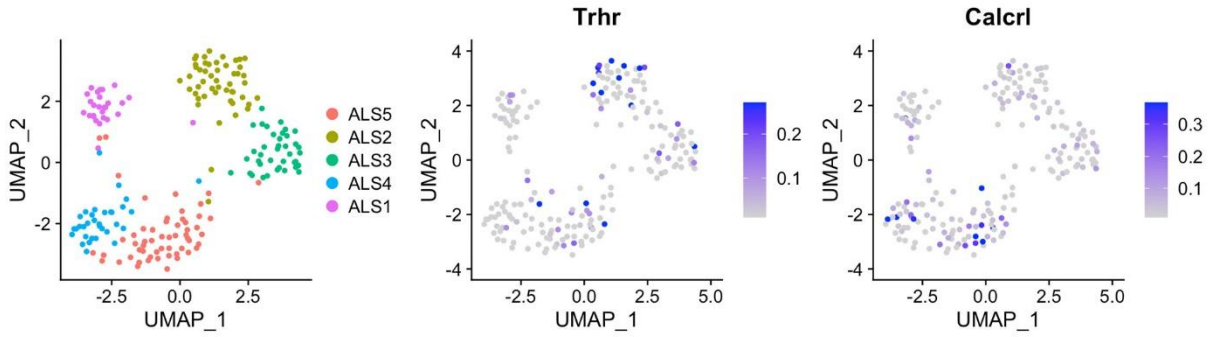

Figure 7–Figure supplement 1 UMAP plot showing the distribution of cells in the ALS1-5 clusters, together with plots for expression of Trhr and Calcrl. Note the presence of both Trhr and Calcrl in several of the ALS clusters, including ALS3.

1523 Table 1 Experimental details for Calb1^{Cre} mice used in anterograde tracing experiments.

1524

Animal	Sex	Injected segments	Injection location	Injection volume (nl)	Viral load (GC)	Survival (days)
1	M	L3, L4, L5	central	300	9.48 x 10^7	26
2	M	L3, L4, L5	central	300	9.48 x 10^7	55
3	F	L3, L4, L5	central	300	9.48 x 10^7	57
4	M	L3	central	300	9.48 x 10^7	42
5	F	L3	central	300	9.48 x 10^7	40
6	F	L3	central	300	9.48 x 10^7	40
7	M	L3, L4, L5	medial	150	4.74 x 10^7	55
8	M	L3, L4, L5	medial	150	4.74 x 10^7	54
9	F	L3, L4, L5	medial	150	4.74 x 10^7	41
10	F	L3, L4, L5	medial	150	4.74 x 10^7	55
11	F	L3	medial	150	4.74 x 10^7	41
12	F	L3	medial	150	4.74 x 10^7	41
13	F	L3	medial	150	4.74 x 10^7	53
14	M	C8	central	500	1.58 x 10^7	35
15	M	C8	central	500	1.58 x 10^7	44
16	M	C8	central	500	1.58 x 10^7	43

1525

1526 Mice received injections of AAV1.Cre^{ON}.tdTomato into the L3 segment only, the L3, L4 and
1527 L5 segments, or the C8 segments on the right side. Injections in lumbar cord were either
1528 targeted centrally (400 µm lateral to the midline) or medially (250 µm lateral to the midline)
1529 within the dorsal horn. Those in cervical cord were located centrally (430-450 µm lateral to

1530 the midline). All injections were made at 300 μm below the surface of the spinal cord.
1531 Injection volume and viral load refer to each injection in animals 1-3 and 7-9.